Rap1-PDZ-GEF1 interacts with a neurotrophin receptor at late endosomes, leading to sustained activation of Rap1 and ERK and neurite outgrowth

Shu Hisata,[1] Toshiaki Sakisaka,[1] Takeshi Baba,[1] Tomohiro Yamada,[1] Kazuhiro Aoki,[2] Michiyuki Matsuda,[2] and Yoshimi Takai[1]

[1]Department of Molecular Biology and Biochemistry, Osaka University Graduate School of Medicine/Faculty of Medicine, Suita 565-0871, Japan
[2]Department of Pathology and Biology of Diseases, Graduate School of Medicine, Kyoto University, Kyoto 606-8501, Japan

Neurotrophins, such as NGF and BDNF, induce sustained activation of Rap1 small G protein and ERK, which are essential for neurite outgrowth. We show involvement of a GDP/GTP exchange factor (GEF) for Rap1, PDZ-GEF1, in these processes. PDZ-GEF1 is activated by GTP-Rap1 via a positive feedback mechanism. Upon NGF binding, the TrkA neurotrophin receptor is internalized from the cell surface, passes through early endosomes, and arrives in late endosomes. A tetrameric complex forms between PDZ-GEF1, synaptic scaffolding molecule and ankyrin repeat-rich membrane spanning protein which interacts directly with the TrkA receptor. At late endosomes, the complex induces sustained activation of Rap1 and ERK, resulting in neurite outgrowth. In cultured rat hippocampal neurons, PDZ-GEF1 is recruited to late endosomes in a BDNF-dependent manner involved in BDNF-induced neurite outgrowth. Thus, the interaction of PDZ-GEF1 with an internalized neurotrophin receptor transported to late endosomes induces sustained activation of both Rap1 and ERK and neurite outgrowth.

Introduction

Formation and extension of axons and dendrites, so-called neurite outgrowth, is a crucial event in neuronal differentiation and maturation during development of the nervous system (Da Silva and Dotti, 2002; Horton and Ehlers, 2003). These morphological changes require reorganization of the cytoskeletal networks and its accompanying membrane expansion and contraction (Craig et al., 1995; Mitchison and Kirschner, 1998). Rap1 small G protein has been shown to be involved in neurite outgrowth and neuronal polarization through regulating the MAPK cascade and the cytoskeletal network (York et al., 1998; Kao et al., 2001; Wu et al., 2001; Schwamborn and Püschel, 2004). Rho small G protein has been shown to be involved in the morphological development of neurons through regulating actin dynamics (Jalink et al., 1993; Kozma et al., 1997; Bito et al., 2000; Da Silva et al., 2003). We previously showed that inactivation of Rho is required for the Rap1-induced neurite outgrowth (Yamada et al., 2005). Rap1-activated Rho GTPase-activating

protein, RA-RhoGAP, transduces a signal from Rap1 to Rho and inactivates Rho. The precise temporary and spatially activation of Rap1 is important for regulating the activity of RA-RhoGAP to produce the neurite. However, the mechanism underlying how and where Rap1 is activated remains unclear.

Neurite outgrowth begins with the activation of membrane receptors of neurotrophins, such as nerve growth factor (NGF) and brain-derived neurotrophic factor (BDNF) (Huang and Reichardt, 2001; Sofroniew et al., 2001; Zweifel et al., 2005). NGF is the prototypic neurotrophin, a group of structurally related signaling proteins that are crucial for the survival, differentiation, and maintenance of specific neuronal population (Snider, 1994). First, NGF binds to TrkA receptor and induces its dimerization, which then activates its own tyrosine kinase and gathers a signaling complex consisting of SOS, a GDP/GTP exchange factor (GEF) specific for Ras small G protein, Grb2, an adaptor protein for SOS, and Shc, a linker protein between Grb2 and TrkA receptor, on the plasma membrane (Kao et al., 2001; Wu et al., 2001). Ras is transiently activated on the plasma membrane and induces activation of the c-Raf-MEK-ERK pathway. On the other hand, activated TrkA receptor gathers another signaling complex consisting of C3G, a GEF specific for Rap1, CrkL, an adaptor protein for C3G, and FRS2, a linker protein

between CrkL and TrkA receptor, on the plasma membrane (Kao et al., 2001; Wu et al., 2001). TrkA receptor and the FRS2-Crk-C3G complex associating with the receptor are internalized into clathrin-coated vesicles and transported to early endosomes (Wu et al., 2001). Rap1 is activated at the early endosomes and induces activation of the B-Raf-MEK-ERK pathway. It has been believed that Rap1 is also activated on the cytoplasmic side of the plasma membrane, but the direct evidence has not been obtained. Then, TrkA receptor proceeds further along the degradative pathway in a microtubule- and motor-dependent fashion, reaching late endosomes, followed by the physical destruction of TrkA receptor by proteolysis in lysosomes (Jullien et al., 2002; Saxena et al., 2005a,b). Thus, transport of TrkA receptor to late endosomes has long been recognized as a means to terminate the signaling via degradation of the activated TrkA receptor complex after their internalization from the cell surface.

Recent studies suggest that TrkA receptor, after binding NGF at the cell surface, passes through early endosomes and reaches to late endosomes within 30 min (Saxena et al., 2005a). However, there is still sustained activation of Rap1 after 30 min (Kao et al., 2001; Wu et al., 2001). Like the activated TrkA receptor complex at early endosomes, TrkA receptor at late endosomes might be competent in the sustained activation of Rap1, but it remains unknown whether, or if so how, Rap1 is activated at late endosomes. Here, we addressed these issues and showed that activated TrkA receptor, which was transported to late endosomes, recruited PDZ-GEF1, a GEF specific for Rap1, by forming a complex through Trk receptors associating ankyrin repeat-rich membrane spanning (ARMS) and synaptic scaffolding molecule (S-SCAM). This tetramer complex then induced the sustained activation of Rap1 and ERK, eventually causing neurite outgrowth. ARMS is a tetraspan transmembrane protein and directly interacts with Trk receptors through each transmembrane domain (Kong et al. 2001; Arevalo et al. 2004). S-SCAM is a synaptic scaffolding molecule with six PDZ domains (Hirao et al., 1998).

Results
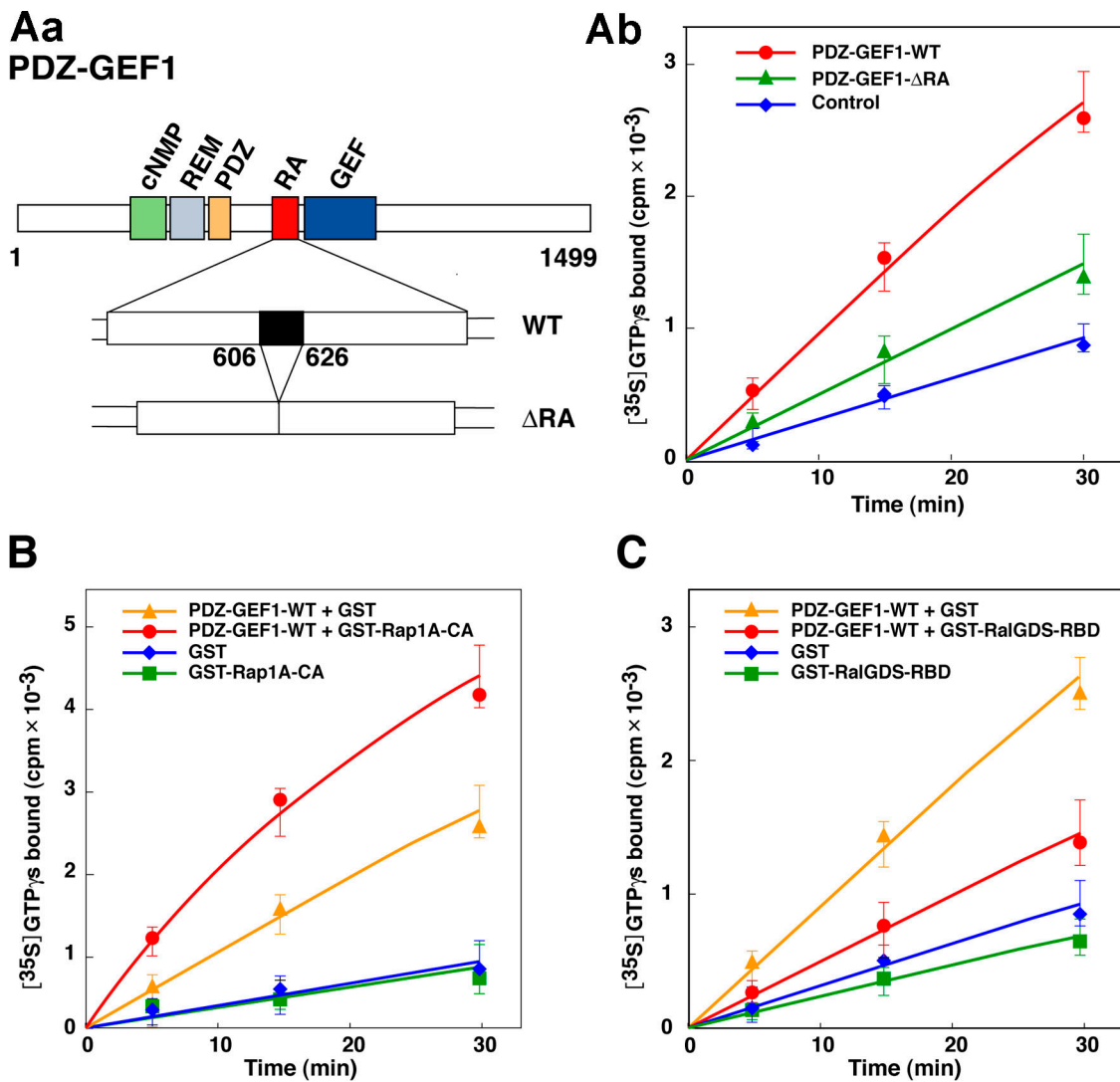
Activation of PDZ-GEF1 by GTP-Rap1

As PDZ-GEF1 has a Rap1-binding RA domain, we first examined whether the binding of GTP-Rap1 to the RA domain affects the GEF activity of PDZ-GEF1. We generated recombinant proteins of FLAG-tagged full-length PDZ-GEF1 (FLAG-PDZ-GEF1) and its RA domain–deficient mutant FLAG-PDZ-GEF1-ΔRA and examined their GEF activity. FLAG-PDZ-GEF1 indeed showed GEF activity toward Rap1 as reported (de Rooij et al., 1999; Liao et al., 1999, 2001; Ohtsuka et al., 1999), while FLAG-PDZ-GEF1-ΔRA showed much less effect on Rap1 (Fig. 1 A). The constitutively active form of GST-Rap1A enhanced the PDZ-GEF1 activity twofold more than control GST did (Fig. 1 B), whereas it did not affect the GEF activity of FLAG-PDZ-GEF1-ΔRA (Fig. S1, available at http://www.jcb.org/cgi/content/full/jcb.200610073/DC1). In addition, GST-Rap-binding domain (RBD) of RalGDS, a specific inhibitor of GTP-Rap1, inhibited the PDZ-GEF1 activity (Fig. 1 C). These results indicate that PDZ-GEF1 is activated by GTP-Rap1 and suggests that once PDZ-GEF1 is activated, its activation is amplified by GTP-Rap1 in a positive feedback mechanism.

Involvement of PDZ-GEF1 in the NGF-induced sustained activation of Rap1 at late endosomes

As PDZ-GEF1 has an auto-amplification GEF activity toward Rap1, we examined whether PDZ-GEF1 is involved in the NGF-induced sustained activation of Rap1 and ERK. We first performed loss-of-function experiments by use of the RNA interference (RNAi) method for PDZ-GEF1. Immunoblotting showed that the amount of PDZ-GEF1 was markedly reduced by the knockdown of PDZ-GEF1 (Fig. 2 A). The amounts of other proteins, including TrkA receptor, another Rap1 GEF C3G, Rap1, Ras, and ERK remained unchanged (unpublished data). The knockdown of PDZ-GEF1 significantly decreased the activation of Rap1, but not Ras, after NGF stimulation as estimated by the pull-down assay (Fig. 2 A and unpublished data). The knockdown of PDZ-GEF1 did not inhibit the activation of ERK at 5 min after NGF stimulation, but it significantly decreased it at 30 and 60 min. The reason why we measured the activation of Rap1 and ERK at 30 and 60 min was that (1) it was reported that activation of Rap1 at 5 min does not contribute to transient activation of ERK at 5 min (York et al., 1998; Kao et al., 2001; Wu et al., 2001; Sasagawa et al., 2005); (2) that a substantial portion of the transient activation of ERK at 5 min mainly depends on Ras, but not on Rap1, whereas the activation of Rap1 at later time points, such as 30 and 60 min, but not at 5 min, contributes to the sustained activation of ERK at 30 and 60 min; and (3) that this sustained activation of ERK is essential for neurite outgrowth.

Consistent with the results of the pull-down assay, the fluorescence resonance energy transfer (FRET) imaging assay showed that the knockdown of PDZ-GEF1 reduced the activation of Rap1 at the perinuclear region of the cells after NGF stimulation (Fig. 2 Ba). To rescue the knockdown of PDZ-GEF1, we generated siRNA-resistant PDZ-GEF1 expression vector (Fig. 2 Bb). Expression of siRNA-resistant PDZ-GEF1 potently rescued the activation of Rap1 at the perinuclear region of the cells at 30 min after NGF stimulation (Fig. 2 Bc). Rap1 has been shown to localize at various intracellular organelles, such as the Golgi complex, early endosomes, and late endosomes, in cultured fibroblasts and epithelial cells (Beranger et al., 1991; Pizon et al., 1994). To examine the localization of endogenous Rap1 in PC12 cells, we performed subcellular fractionation from the post-nuclear supernatant (PNS) of PC12 cells. A significant amount of Rap1 was recovered in the EEA1-positive early endosomal fraction and the Rab7-positive late endosomal fraction (Fig. 2 Ca). To examine the localization of GTP-Rap1 in PC12 cells, we performed the subcellular fractionation in the presence of GST-RalGDS-3xRBD, which preferentially binds to GTP-Rap1 (Herrmann et al., 1996). GST-RalGDS-3xRBD was recovered in the late endosomal fraction at 30 min after NGF stimulation, indicating that Rap1 was activated at late endosomes at 30 min after NGF stimulation (Fig. 2 Cb). The huge amount of GST- RalGDS-3xRBD, which did not bind to Rap1, remained in the bottom PNS and heavy membrane fractions.

The NGF-induced neurite outgrowth was reduced in the PDZ-GEF1-knockdown PC12 cells (Fig. 2 D). This knockdown effect was rescued by expression of siRNA-resistant PDZ-GEF1 (Fig. 2 E). Moreover, PC12 cells overexpressing PDZ-GEF1 or

Figure 1. **Activation of PDZ-GEF1 by GTP-Rap1.** (A) Requirement of the RA domain for full activation of PDZ-GEF1. (Aa) Schematic structures of PDZ-GEF1 and its RA domain–deficient mutant (PDZ-GEF1-ΔRA). (Ab) GEF activities of PDZ-GEF1 and PDZ-GEF1-ΔRA. GDP-Rap1A was incubated with FLAG-PDZ-GEF1, FLAG-PDZ-GEF1-ΔRA, or buffer (Control) in the presence of [^{35}S]GTPγS for indicated periods of time. (B) Enhancement of the GEF activity of PDZ-GEF1 by Rap1A. GDP-Rap1A was incubated with both FLAG-PDZ-GEF1 and GST-V12Rap1A (GST-Rap1A-CA), both FLAG-PDZ-GEF1 and GST, GST-Rap1A-CA alone, or GST alone, in the presence of [^{35}S]GTPγS for indicated periods of time. (C) Inhibition of the GEF activity of PDZ-GEF1 by the Rap1-binding domain of RalGDS (RalGDS-RBD). GDP-Rap1A was incubated with both FLAG-PDZ-GEF1 and GST-RalGDS-RBD, both FLAG-PDZ-GEF1 and GST, GST-RalGDS-RBD alone, or GST alone, in the presence of [^{35}S]GTPγS for indicated periods of time. The radioactivity of [^{35}S]GTPγS bound to Rap1A was scintillation-counted and plotted. The results shown are representative of three independent experiments.

PDZ-GEF1-ΔRA displayed marked neurite outgrowth at 12 h after NGF stimulation as compared with control cells (Fig. S2, available at http://www.jcb.org/cgi/content/full/jcb.200610073/DC1). Consistent with the difference in the GEF activities between PDZ-GEF1 and PDZ-GEF1-ΔRA shown in Fig. 1 Ab, the effect of PDZ-GEF1-ΔRA on neurite outgrowth was less effective than that of PDZ-GEF1. Collectively, these results indicate that PDZ-GEF1 is involved in the NGF-induced sustained activation of Rap1 and ERK, which eventually causes neurite outgrowth.

Before NGF stimulation, FLAG-PDZ-GEF1 diffusely localized at the cytoplasm, but it was recruited to LBPA-positive late endosomes at 30 min after NGF stimulation (Fig. 3). FLAG-PDZ-GEF1 was not recruited to EEA1-positive early endosomes at either 5 or 30 min. In contrast to PDZ-GEF1, C3G was recruited

to EEA1-positive early endosomes at 5 min after NGF stimulation (Fig. S3, available at http://www.jcb.org/cgi/content/full/jcb.200610073/DC1). C3G was not recruited to LBPA-positive late endosomes at either 5 or 30 min. These results indicate that PDZ-GEF1 is recruited to late endosomes in response to NGF and suggest that this Rap1 GEF is involved in the NGF-induced sustained activation of Rap1 at late endosomes.

Involvement of transport of TrkA receptor to late endosomes in the NGF-induced recruitment of PDZ-GEF1

We next examined whether transport of TrkA receptor to late endosomes recruits PDZ-GEF1 there. Bafilomycin is known to be an inhibitor of V-ATPase–regulating protein trafficking from
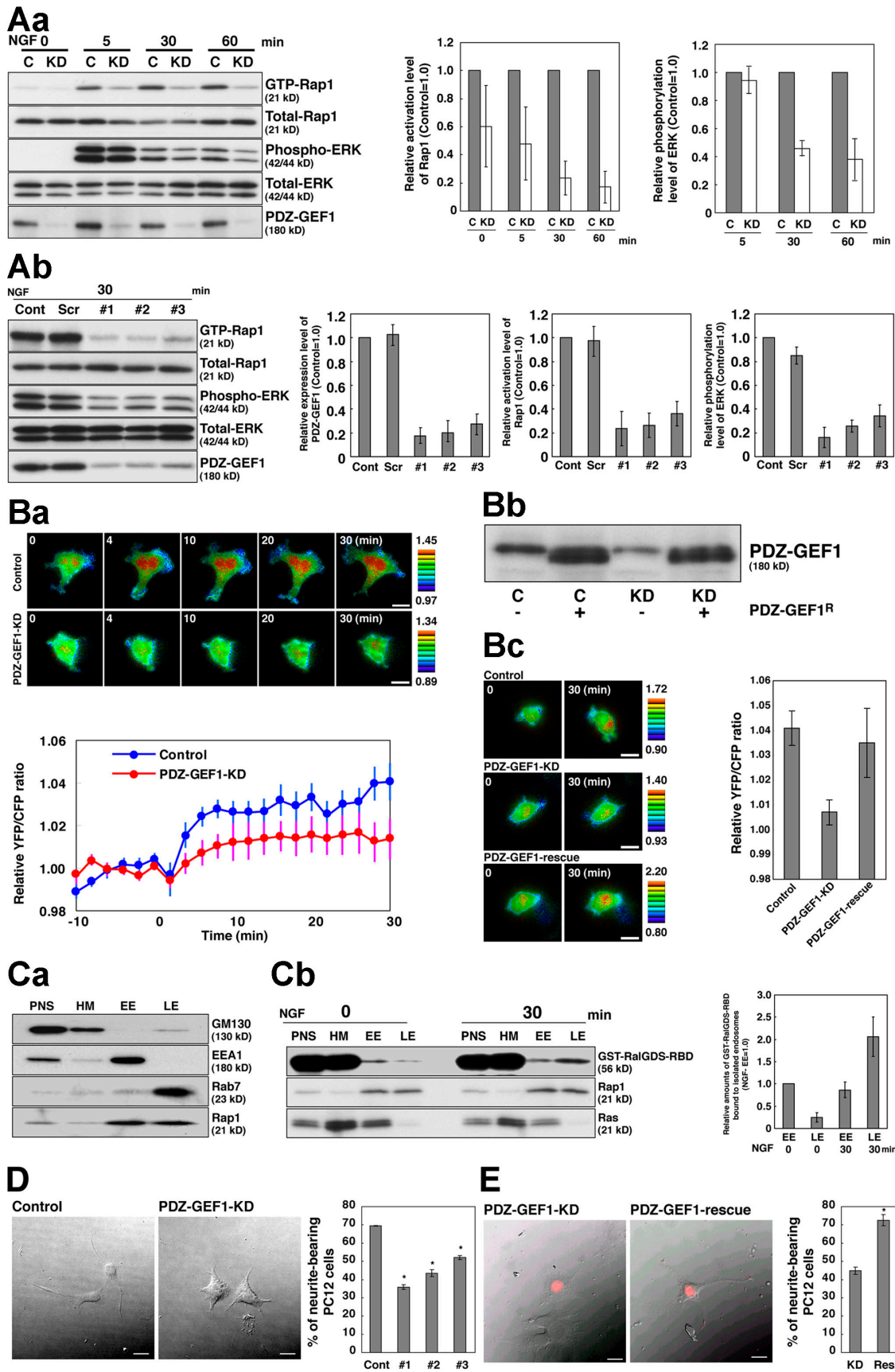
Figure 2. **Involvement of PDZ-GEF1 in the NGF-induced sustained activation of Rap1 and neurite outgrowth in PC12 cells.** (A) The activation level of Rap1 and the phosphorylation level of ERK in PC12 cells. (Aa) Effects of the knockdown of PDZ-GEF1 on the activation of Rap1 and ERK after NGF stimulation
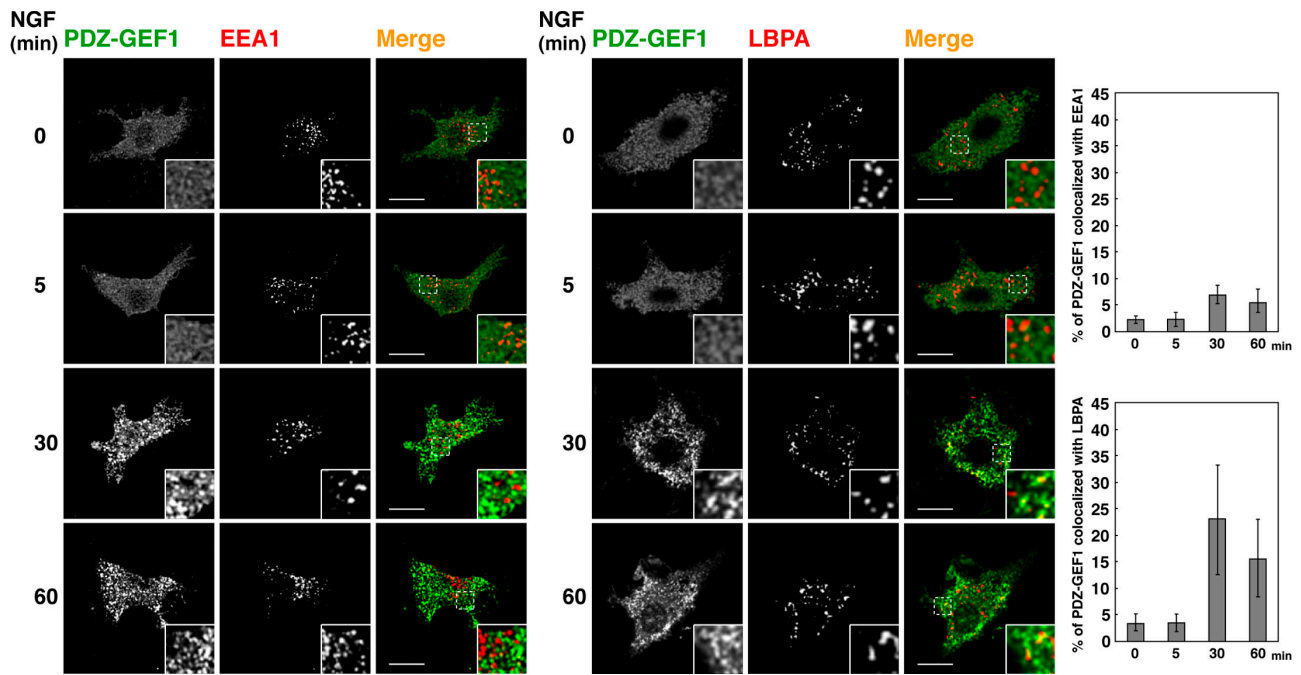
Figure 3. **Recruitment of PDZ-GEF1 to late endosomes in a NGF-dependent manner.** PC12 cells were transfected with pFLAG-CMV2-PDZ-GEF1. PC12 cells were double-stained with the anti-PDZ-GEF pAb and the anti-EEA1 mAb (left panels) or with the anti-PDZ-GEF pAb and the anti-LBPA mAb (right panels). Insets are enlarged images of boxed areas. The area of colocalization was quantified in the right panel. Bars, 10 μm. The results shown are representative of three independent experiments.

early to late endosomes (Hurtado-Lorenzo et al., 2006). The immunofluorescence signal for TrkA receptor became concentrated at EEA1-positive early endosomes at 5 min and at LBPA-positive late endosomes at 30 min after NGF stimulation (Fig. S4, available at http://www.jcb.org/cgi/content/full/jcb.200610073/DC1). Bafilomycin did not inhibit the NGF-induced transport of TrkA receptor to EEA1-positive early endosomes at 5 min, but it significantly decreased the transport of TrkA receptor to LBPA-positive late endosomes at 30 min (Fig. 4 A and Fig. S4). Bafilomycin inhibited the recruitment of PDZ-GEF1 to LBPA-positive

late endosomes at 30 min after NGF stimulation (Fig. 4 B). These results indicate that transport of TrkA receptor to late endosomes is required for the recruitment of PDZ-GEF1 to late endosomes.

Bafilomycin inhibited the activation of Rap1 at 5 min and more potently at 30 and 60 min as estimated by the pull-down assay (Fig. 4 Ca). In contrast, bafilomycin did not inhibit the activation of Ras at 5 min (Fig. 4 Cb). Bafilomycin did not inhibit the activation of ERK at 5 min, but significantly decreased it at 30 and 60 min. Bafilomycin reduced the NGF-induced activation of Rap1 at the perinuclear region of the cells as estimated

in PC12 cells. PC12 cells were transfected with control RNA (C) or PDZ-GEF1 siRNA #1 (KD). The amount of GTP-Rap1 was measured by the pull-down assay using GST-RalGDS. The amount of phospho-ERK was measured by immunoblotting with the anti-phospho-ERK mAb. The immunoblot bands were quantified in the right panel. (Ab) Effects of three PDZ-GEF1 siRNAs and scramble RNA on the activation of Rap1 and ERK. The immunoblot bands were quantified in the right panel. (B) FRET analysis on the localization of the activation of Rap1 in PC12 cells. (Ba) FRET analysis in PDZ-GEF1-knockdown PC12 cells. PC12 cells were transfected with an empty pSUPER-retro vector (Control) or pSUPER-retro-PDZ-GEF1 (PDZ-GEF1-KD). In the top panel, representative ratio images of YFP/CFP at indicated time points after NGF stimulation are shown. In the intensity-modulated display mode, eight colors from red to blue were used to represent the YFP/CFP ratio, with the intensity of each color indicating the mean intensity of YFP and CFP. The upper and lower limits of the ratio range are shown in the right panel. Bars, 10 μm. In the bottom panel, YFP/CFP ratios of three representative datasets were expressed by measuring the increase over the reference value used in the top panel. (Bb) Expression of FLAG-siRNA-resistant PDZ-GEF1 in PDZ-GEF1-knockdown PC12 cells. PC12 cells were first transfected with PDZ-GEF1 siRNA #1 (KD) or scramble RNA (C) and cultured for a day. Then cells were transfected with pERed NLS-FLAG vector or pERed NLS-FLAG-siRNA resistant PDZ-GEF1 and cultured for a day. The total cell lysates were subjected to SDS-PAGE, followed by immunoblotting with the anti-PDZ-GEF1 pAb. (Bc) FRET analysis in rescued PDZ-GEF1-knockdown PC12 cells. Representative ratio images of YFP/CFP at 30 min after NGF stimulation are shown. In the right panel, YFP/CFP ratios of three representative datasets were expressed by measuring the increase over the reference value obtained from the cells before NGF stimulation. (C) Localization of endogenous Rap1 and GTP-Rap1 in PC12 cells. (Ca) Localization of endogenous Rap1 in PC12 cells. The PNS fraction from PC12 cells was subjected to sucrose gradient centrifugation. Equal amounts of proteins from different fractions were subjected to immunoblotting with indicated Abs. PNS; post-nuclear supernatant fraction, HM; heavy membrane fraction, EE; early endosomal fraction, LE; late endosomal fraction. (Cb) Localization of GTP-Rap1 in PC12 cells. The PNS fraction from PC12 cells stimulated with or without NGF for 30 min was incubated with GST-RalGDS-3xRBD and subjected to sucrose gradient centrifugation. Equal amounts of proteins from different fractions were subjected to immunoblotting with indicated Abs. The immunoblot bands were quantified in the right panel. (D) Neurite outgrowth in the NGF-treated PC12 cells. PC12 cells were transfected with control scramble siRNA (Control) or PDZ-GEF1 siRNA#1-3 (PDZ-GEF1-KD). Left panel: representative DIC images. Right panel: percentage of cells with neurites. (E) Rescue of the inhibitory effect of the knockdown of PDZ-GEF1 on the neurite outgrowth. PC12 cells were transfected with pSUPER-retro-PDZ-GEF1 and pERed NLS-FLAG vector (PDZ-GEF1-KD) or pSUPER-retro-PDZ-GEF1 and pERed NLS-FLAG siRNA-resistant PDZ-GEF1 (PDZ-GEF1-rescue). Left panel: representative DIC images. Right panel: percentage of cells with neurites. Asterisks indicate statistical significance (t test; *, $P < 0.01$). Bars, 10 μm. The results shown are representative of three independent experiments.
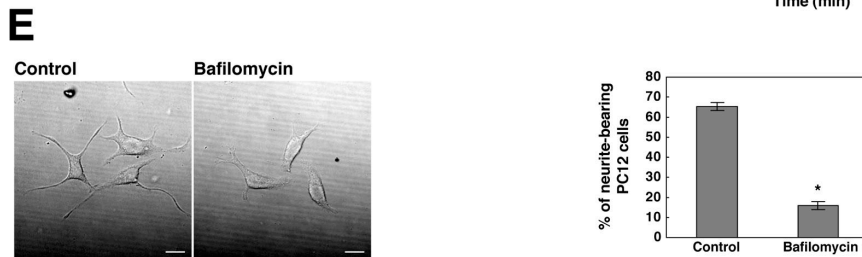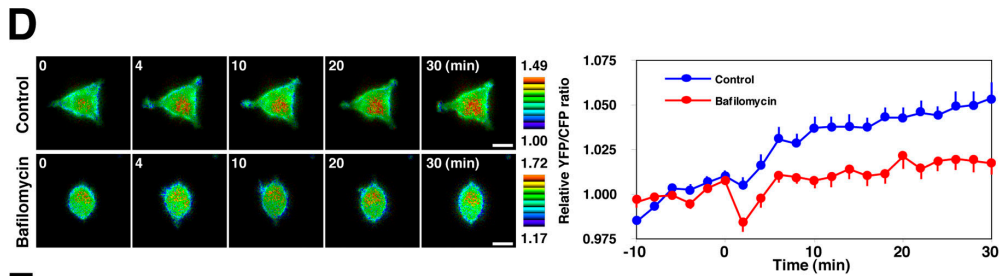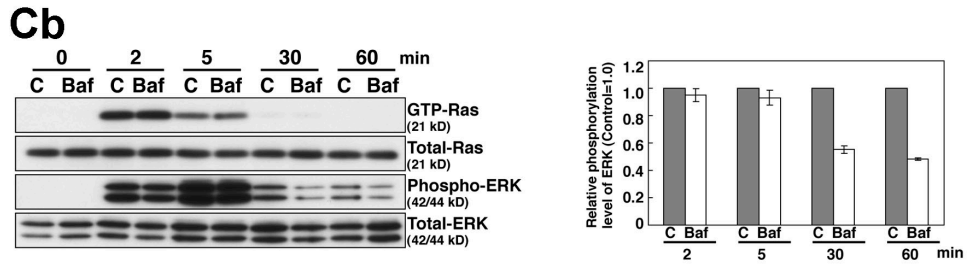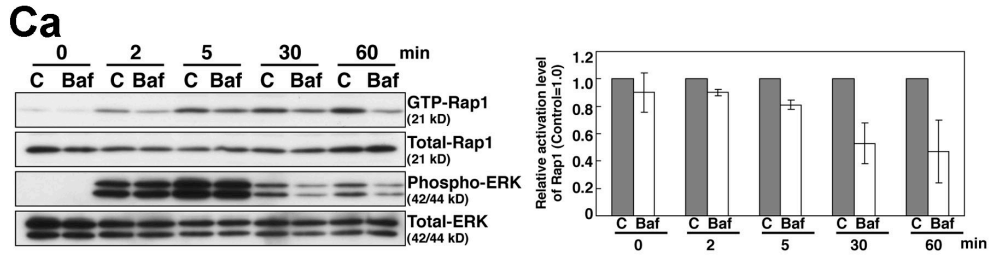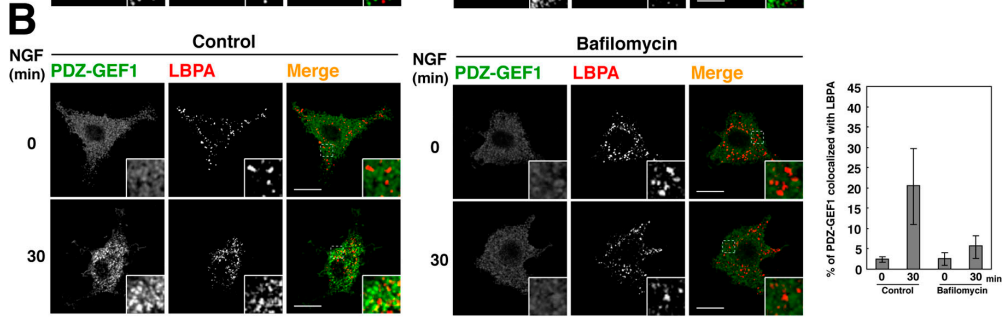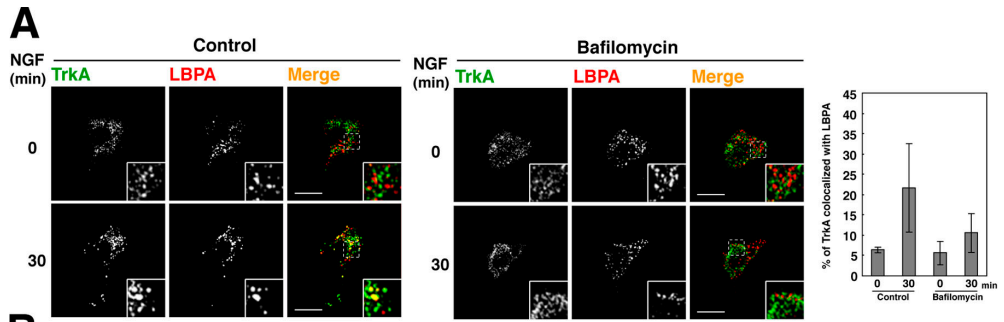
by the FRET assay (Fig. 4 D). Bafilomycin reduced the NGF-induced neurite outgrowth (Fig. 4 E). Collectively, these results indicate that the NGF-induced internalization and transport of TrkA receptor to late endosomes is involved in the NGF-induced sustained activation of Rap1 and ERK and neurite outgrowth by recruiting PDZ-GEF1 to late endosomes.

NGF-induced formation of a tetramer complex of PDZ-GEF1, S-SCAM, ARMS, and TrkA receptor

We next attempted to understand the molecular mechanism how PDZ-GEF1 induces the activation of Rap1 at late endosomes in response to NGF. We previously showed that PDZ-GEF1 directly binds S-SCAM (Ohtsuka et al., 1999), whereas it was shown that TrkA receptor directly binds an endosomal protein ARMS (Yano and Chao, 2005; Arevalo et al. 2006). Consistent with our earlier observation, S-SCAM was coimmunoprecipitated with PDZ-GEF1 before or after NGF stimulation (Fig. 5 A). ARMS and TrkA receptor were also coimmunoprecipitated with PDZ-GEF1, but this coimmunoprecipitation was strengthened after NGF stimulation. However, presumably due to the reconstitution of the complex during the procedure of cell lysis, we did not get the strong difference in the amount of the complex between 5 min and 60 min after NGF stimulation. These results suggest that PDZ-GEF1 forms a tetramer complex with S-SCAM, ARMS, and TrkA receptor after NGF stimulation.

As ARMS has a PDZ-binding motif, RESIL, at the cytoplasmic tail, we examined by the pull-down assay whether ARMS directly binds to S-SCAM or PDZ-GEF1. The GST fusion protein containing the C-terminal region of ARMS (GST-ARMS-C-terminal) bound to S-SCAM, but not to PDZ-GEF1 (Fig. 5 B and unpublished data). GST-ARMS-C-terminal lacking the last three amino acids in the RESIL motif (GST-ARMS-C-terminal-ΔSIL) did not bind to S-SCAM. The PDZ4 domain of S-SCAM bound to GST-ARMS-C-terminal (Fig. 5 C, a and b). Under the conditions where Myc-S-SCAM was coimmunoprecipitated with FLAG-ARMS, Myc-S-SCAM lacking the PDZ4 domain (S-SCAM-ΔPDZ4) was not coimmunoprecipitated (Fig. 5 Cc). These results indicate that S-SCAM directly binds ARMS and that this binding is mediated by the PDZ4 domain of S-SCAM and the PDZ-binding motif of ARMS. Collectively with the earlier observations that PDZ-GEF1 binds to the PDZ1 domain of S-SCAM and that ARMS directly binds to TrkA receptor in a NGF-dependent manner, these results indicate that PDZ-GEF1 binds to S-SCAM to form a binary complex in a NGF-independent manner, which binds to TrkA receptor through ARMS to form a tetramer complex in a NGF-dependent manner.

### Formation of the tetramer complex at late endosomes

We then examined whether this tetramer complex of PDZ-GEF1, S-SCAM, ARMS, and TrkA receptor is formed at late endosomes in intact PC12 cells. The immunofluorescence signal for ARMS was mainly concentrated at LBPA-positive late endosomes, not at early endosomes, before and after NGF stimulation, indicating that ARMS is an intrinsic late endosomal protein (Fig. 6 A). The signals for PDZ-GEF1 and S-SCAM localized diffusely at the cytoplasm before NGF stimulation (Fig. 6 B, a and c). The signal for TrkA receptor localized at the cell surface plasma membrane and a vesicular-like structure, presumably, early endosomes, before NGF stimulation (Fig. 6 Bb). The signals for PDZ-GEF1, S-SCAM, and TrkA receptor became concentrated at ARMS-positive late endosomes after NGF stimulation. As the signals for PDZ-GEF1 and S-SCAM colocalized well before and after NGF stimulation, these two molecules seem to form a binary complex, consistent with the above coimmunoprecipitation results (Fig. S5A, available at http://www.jcb.org/cgi/content/full/jcb.200610073/DC1). Collectively, these results suggest that upon binding of NGF, TrkA receptor is internalized and transported to ARMS-positive late endosomes, interacts with ARMS, and then recruits the PDZ-GEF1-S-SCAM complex mainly to ARMS-positive late endosomes, resulting in the tetramer complex formation.

To further examine the recruitment of PDZ-GEF1 to late endosomes biochemically, we performed immunoisolation of PDZ-GEF1-containing vesicles using PDZ-GEF1 pAb-coated magnetic beads from the PNS fraction from NGF- nonstimulated and -stimulated PC12 cells. Rab7 was recovered in the immunoisolated PDZ-GEF1-containing vesicles, whereas EEA1 was not recovered in the immunoisolated vesicles (Fig. 6 Bd). Rab7 and ARMS were more predominantly recovered after NGF stimulation. These results have provided another line of evidence that the tetramer complex of TrkA receptor, ARMS, S-SCAM, and PDZ-GEF1 is formed mainly at late endosomes in a NGF-dependent manner.

Necessity of ARMS and S-SCAM for the NGF-induced recruitment of PDZ-GEF1 to late endosomes and neurite outgrowth

To confirm that ARMS and S-SCAM are required for the recruitment of PDZ-GEF1 to late endosomes, we performed

---

Figure 4. **Involvement of the transport of TrkA receptor to late endosomes in the NGF-induced recruitment of PDZ-GEF1.** (A) Inhibition of the transport of TrkA receptor from early endosomes to late endosomes by bafilomycin. Serum-starved PC12 cells were treated with bafilomycin for 2 h and stimulated by NGF for 30 min. PC12 cells were double-stained with the anti-TrkA receptor pAb and the anti-LBPA mAb. Insets are enlarged images of boxed areas. The area of colocalization was quantified in the right panel. Bars, 10 μm. (B) Inhibition of the recruitment of PDZ-GEF1 to late endosomes by bafilomycin. PC12 cells were transfected with pFLAG-CMV2-PDZ-GEF1. PC12 cells were double-stained with the anti-PDZ-GEF1 pAb and the anti-LBPA mAb. The area of colocalization was quantified in the right panel. (C) Effect of bafilomycin on the NGF-induced activation of Ras, Rap1, and ERK. (Ca) Inhibitory effect of bafilomycin on the NGF-induced activation of Rap1. Serum-starved PC12 cells were treated with DMSO (C) or bafilomycin (Baf) and stimulated by NGF for indicated periods of time. The immunoblot bands were quantified in the right panel. (Cb) No effect of bafilomycin on the NGF-induced activation of Ras. The immunoblot bands were quantified in the right panel. (D) The localization of the activation of Rap1 in PC12 cells by FRET analysis. In the left panel, representative ratio images of YFP/CFP at indicated time points after NGF stimulation are shown as described in Fig. 2 Ba. In the right panel, YFP/CFP ratios of three representative datasets were expressed by measuring the increase over the reference value obtained from the cells before NGF stimulation. Bars, 10 μm. (E) Inhibition of neurite outgrowth by bafilomycin. Left panel: representative DIC images. Right panel: percentage of cells with neurites. Asterisks indicate statistical significance (*t* test; *, P < 0.01). Bars, 10 μm. The results shown are representative of three independent experiments.
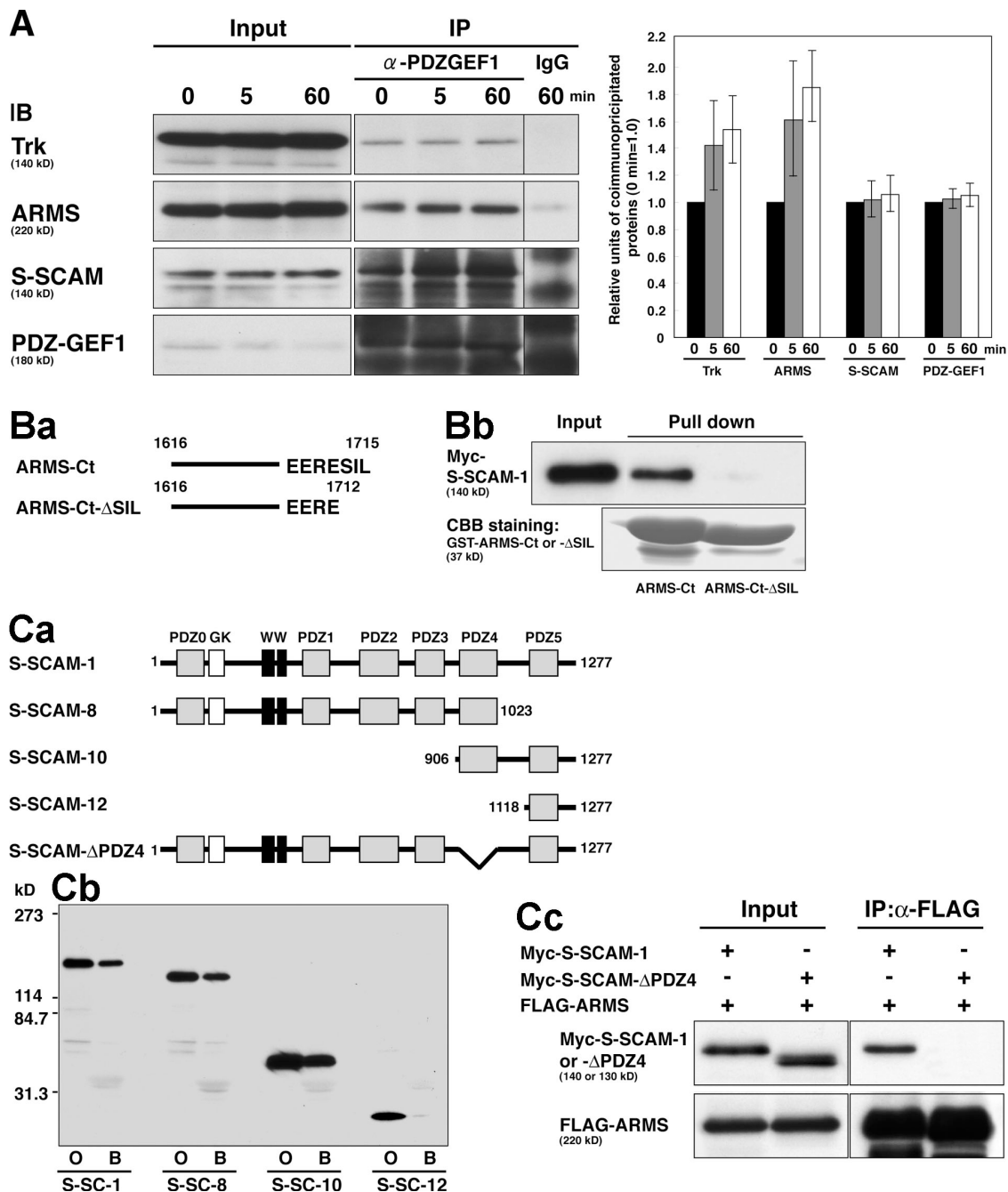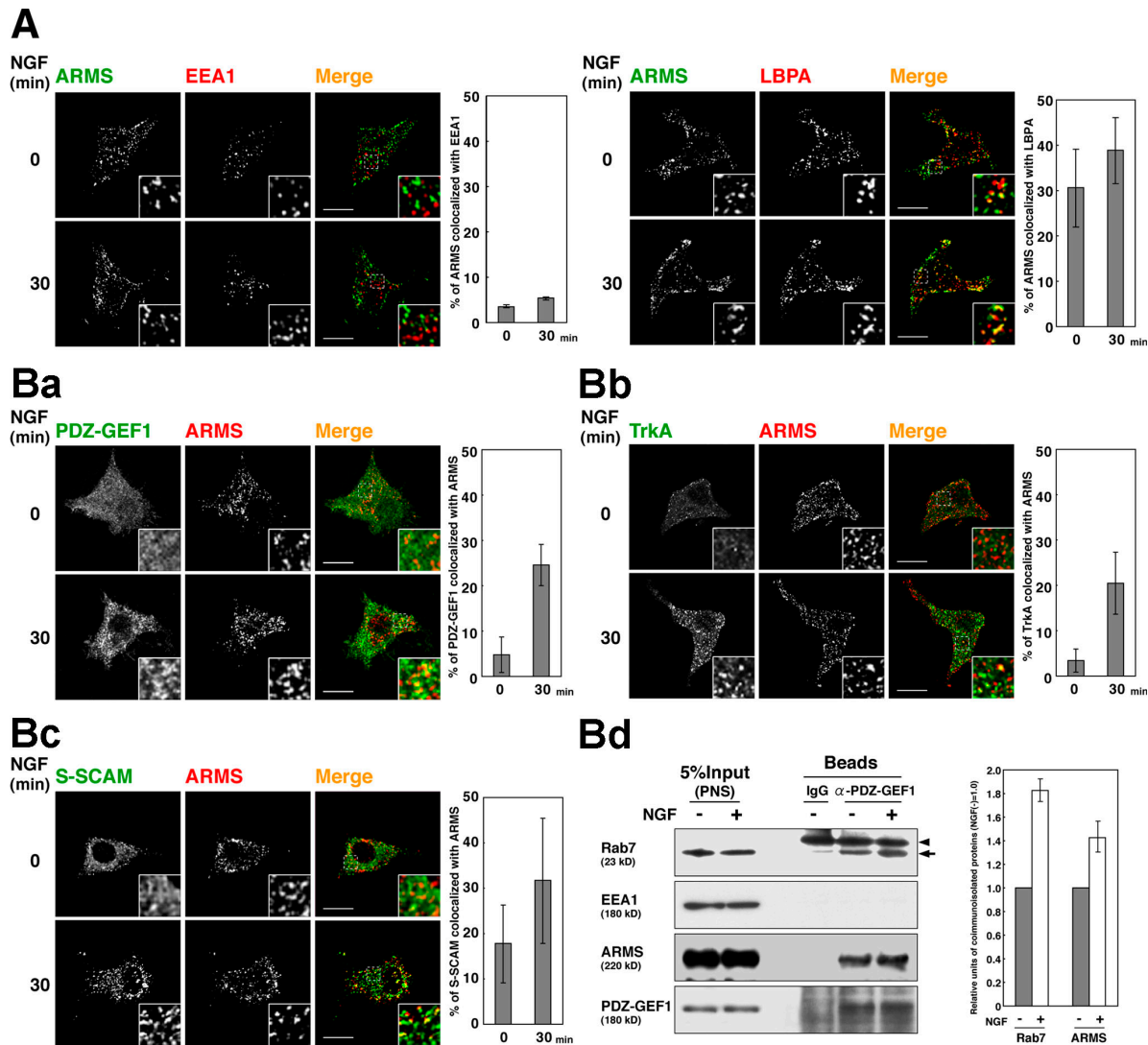
Figure 5. **Formation of the ARMS-S-SCAM-PDZ-GEF1 complex in a NGF-dependent manner.** (A) Co-immunoprecipitation of PDZ-GEF1 with S-SCAM, ARMS, and Trk receptor from PC12 cells. PC12 cells were stimulated by NGF for indicated periods of time. The extract of PC12 cells was immunoprecipitated with the anti-PDZ-GEF1 pAb and immunoblotted with indicated Abs. The immunoblot bands were quantified in the right panel. (B) Binding of ARMS to S-SCAM through its C-terminal tail SIL. (Ba) Schematic depiction of C-terminal of ARMS (ARMS-Ct) and its SIL-deletion mutant (ARMS-Ct-ΔSIL). (Bb) Pull-down assay. The extract of HEK293 cells expressing Myc-S-SCAM was incubated with GST-ARMS-Ct or GST-ARMS-Ct-ΔSIL immobilized on glutathione-Sepharose beads. The bound proteins were analyzed by immunoblotting with the anti-Myc mAb. GST fusion proteins were immobilized in comparable quantities (bottom; Coomassie brilliant blue [CBB] staining). (C) Binding of S-SCAM to ARMS through its PDZ4 domain. (Ca) Schematic depiction of various truncated forms of S-SCAM. (Cb) Pull-down assay. The extract of HEK293 cells expressing various truncated forms of Myc-S-SCAM was incubated with GST-ARMS-Ct immobilized on glutathione-Sepharose beads. The bound proteins were analyzed by immunoblotting with the anti-Myc mAb. O, original cell extract; B, bound proteins. (Cc) Co-immunoprecipitation assay. HEK293 cells were cotransfected with both FLAG-ARMS and Myc-S-SCAM or both FLAG-ARMS and Myc-S-SCAM-ΔPDZ4. The extract of HEK293 cells was incubated with the anti-FLAG mAb. The immunoprecipitates were analyzed by immunoblotting with the anti-Myc pAb and anti-FLAG pAb. The results shown are representative of three independent experiments.

loss-of-function experiments by use of the RNAi method for ARMS or by use of a dominant negative mutant for S-SCAM. The recruitment of FLAG-PDZ-GEF1 to late endosomes was reduced in the ARMS-knockdown PC12 cells (Fig. 7, A and B, and Fig. S5 B). Expression of Myc-S-SCAM did not inhibit the recruitment of FLAG-PDZ-GEF1 to late endosomes, but expression of

Figure 6. **Localization of the ARMS-S-SCAM-PDZ-GEF1 complex at late endosomes in a NGF-dependent manner.** (A) Localization of ARMS at the late endosomes. PC12 cells were stimulated by NGF for 30 min and double-stained with the anti-ARMS pAb and the anti-EEA1 mAb or with the anti-ARMS pAb and the anti-LBPA mAb. Insets are enlarged images of boxed areas. The area of colocalization was quantified in the right panel. Bars, 10 μm. (B) Recruitment of PDZ-GEF1, S-SCAM, and TrkA receptor to ARMS-positive late endosomes. (Ba) Recruitment of PDZ-GEF1 to ARMS-positive late endosomes. PC12 cells were transfected with pFLAG-CMV2-PDZ-GEF1. PC12 cells were double-stained with the anti-PDZ-GEF pAb and the anti-ARMS mAb. The area of co-localization was quantified in the right panel. (Bb) Recruitment of TrkA receptor to ARMS-positive late endosomes. PC12 cells were double-stained with the anti-TrkA receptor pAb and the anti-ARMS mAb. The area of colocalization was quantified in the right panel. (Bc) Recruitment of S-SCAM to ARMS-positive late endosomes. PC12 cells were double-stained with the anti-S-SCAM pAb and the anti-ARMS mAb. The area of colocalization was quantified in the right panel. (Bd) Immunoisolation of PDZ-GEF1-containing vesicles. PDZ-GEF1-containing vesicles were immunoisolated with the anti-PDZ-GEF1 pAb or the anti–rabbit IgG (control IgG)-coated magnetic beads from the PNS fraction of PC12 cells. The bound proteins were analyzed by immunoblotting with indicated Abs. Arrowhead indicates a light chain of rabbit IgG. Arrow indicates Rab7. The PDZ-GEF1-pAb immunoreactive nonspecific bands were observed in the control IgG coated-magnetic beads presumably due to the nonspecific reaction of the secondary Ab against the contaminating proteins interacted with the magnetic beads. The immunoblot bands were quantified in the right panel. The results were obtained from the same experiments and the same gels. The results shown are representative of three independent experiments.

Myc-S-SCAM-ΔPDZ4 reduced the recruitment of FLAG-PDZ-GEF1 to late endosomes (Fig. 7 C). Expression of Myc-S-SCAM, but not Myc-S-SCAM-ΔPDZ4, slightly induced the recruitment of FLAG-PDZ-GEF1 to late endosomes even in the absence of NGF (Fig. S5A).

We next examined whether ARMS and S-SCAM are indeed involved in the NGF-induced neurite outgrowth. The NGF-induced neurite outgrowth was reduced in the ARMS-knockdown PC12 cells (Fig. 7 D). The NGF-induced neurite outgrowth was reduced in the PC12 cells expressing Myc-S-SCAM-ΔPDZ4

(Fig. 7 E). Collectively, these results indicate that ARMS and S-SCAM are essential for the NGF-induced recruitment of PDZ-GEF1 to late endosomes and neurite outgrowth.

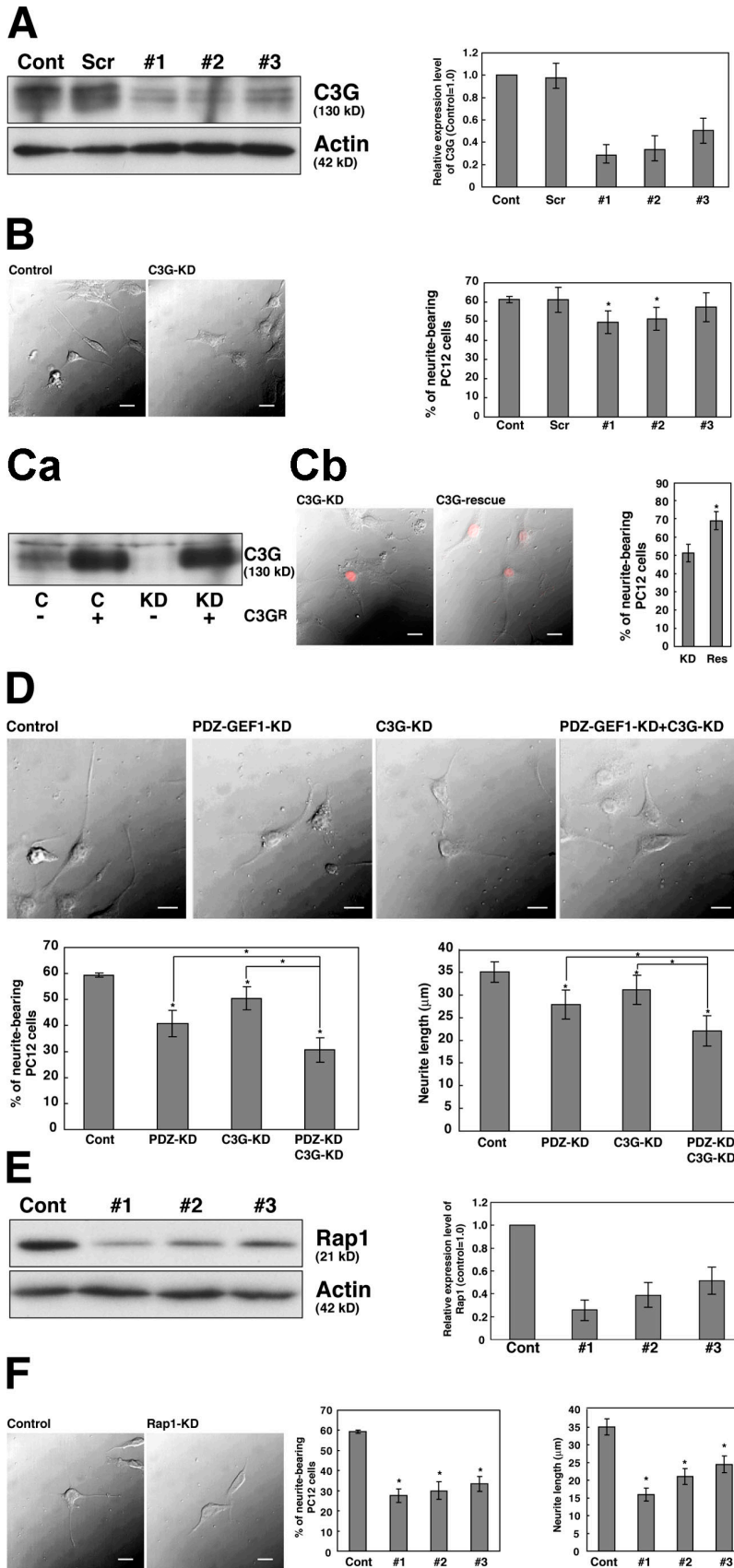### Involvement of C3G and PDZ-GEF1 in the NGF-induced neurite outgrowth

To understand the relationship between C3G and PDZ-GEF1 in the NGF-induced neurite outgrowth, we first performed loss-of-function experiments by use of the RNAi method for C3G (Fig. 8 A). The inhibitory effect of the knockdown of C3G on
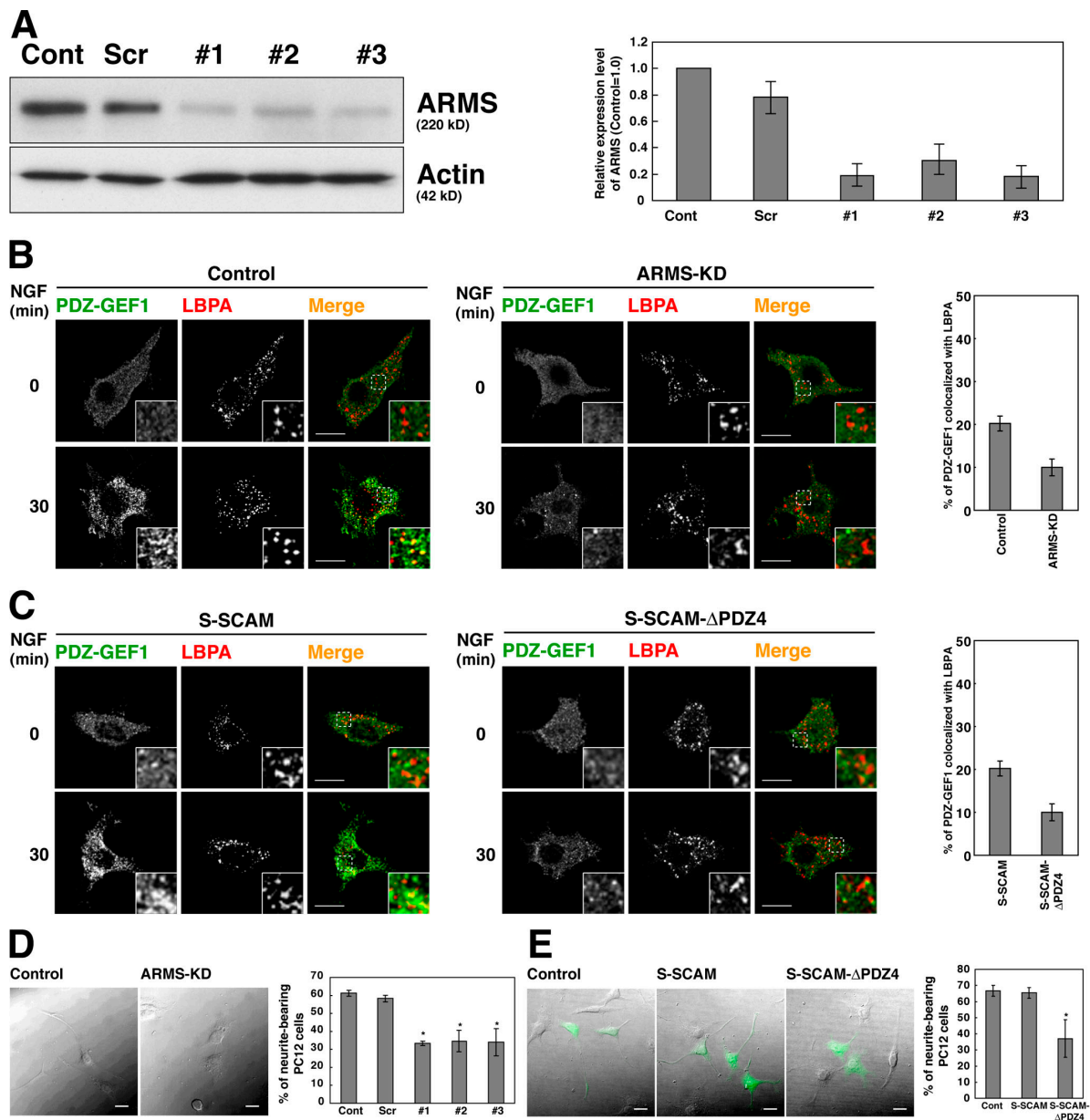
Figure 7. **Requirement of ARMS and S-SCAM for recruiting PDZ-GEF1 to late endosomes.** (A) Efficiency of the knockdown of ARMS by three different siRNAs. PC12 cells were transfected with control siRNA (Cont), ARMS siRNAs #1-3, or scramble RNA (Scr). The immunoblot bands were quantified in the right panel. (B) Requirement of ARMS for recruiting PDZ-GEF1 to late endosomes. PC12 cells were cotransfected with both pFLAG-CMV2-PDZ-GEF1 and scramble control siRNA (Control) or with both pFLAG-CMV2-PDZ-GEF1 and ARMS siRNA (ARMS-KD). Cells were stimulated by NGF for 30 min and double-stained with the anti-PDZ-GEF1 pAb and the anti-LBPA mAb. Insets are enlarged images of boxed areas. The area of colocalization was quantified in the right panel. (C) Requirement of PDZ4 domain of S-SCAM for recruiting PDZ-GEF1 to late endosomes. PC12 cells were cotransfected with both pFLAG-CMV2-PDZ-GEF1 and pCIneo-Myc-S-SCAM or with pFLAG-CMV2-PDZ-GEF1 and pCIneo-Myc-S-SCAM-ΔPDZ4. Transfected PC12 cells were stimulated by NGF for 30 min and double-stained with the anti-PDZ-GEF1 pAb and the anti-LBPA mAb. The area of colocalization was quantified in the right panel. (D) Inhibition of neurite outgrowth in the AMRS-knockdown PC12 cells. PC12 cells were transfected with scramble control siRNA (Control) or ARMS siRNA #1-3 (ARMS-KD). Left panel: representative DIC images. Right panel: percentage of cells with neurites. (E) Inhibition of neurite outgrowth in PC12 cells expressing S-SCAM-ΔPDZ4. PC12 cells were transfected with GFP (Control) or cotransfected with GFP as a morphological marker along with pCIneo-Myc-S-SCAM or pCIneo-Myc-S-SCAM-ΔPDZ4. Left panel: representative DIC images. Right panel: percentage of cells with neurites. Asterisks indicate statistical significance (*t* test; *, P < 0.05). Bars, 10 μm. The results shown are representative of three independent experiments.

neurite outgrowth was less effective than that of the knockdown of PDZ-GEF1 (Fig. 8 B). Consistently, overexpression of C3G enhanced the NGF-induced neurite outgrowth less effectively than that of PDZ-GEF1 (Fig. S2). The effect of the knockdown of C3G was rescued by expression of siRNA-resistant C3G (Fig. 8 C). The double knockdown of C3G and PDZ-GEF1 reduced neurite

outgrowth more potently than the knockdown of PDZ-GEF1 or C3G alone (Fig. 8 D). In addition, the inhibitory effect of the double knockdown of C3G and PDZ-GEF1 on neurite outgrowth was similar to that of the knockdown of Rap1 (Fig. 8, E and F). These results indicate C3G and PDZ-GEF1 are main Rap1GEFs in the NGF-induced neurite outgrowth in PC12 cells.

Figure 8. **Involvement of C3G and PDZ-GEF1 in the NGF-induced neurite outgrowth.** (A) Efficiency of the knockdown of C3G by three different siRNAs. PC12 cells were transfected with control siRNA (Cont), C3G siRNAs #1-3, or scramble RNA (Scr). The immunoblot bands were quantified in the right panel. (B) Inhibition of neurite outgrowth in the C3G-knockdown PC12 cells. PC12 cells were transfected with scramble RNA (Control) or C3G siRNA #1-3 (C3G-KD). Left panel: representative DIC images. Right panel: percentage of cells with neurites. (C) Rescue of the inhibitory effect of the knockdown of C3G on neurite outgrowth. (Ca) Expression of FLAG-siRNA-resistant C3G in the C3G-knockdown PC12 cells. PC12 cells were first transfected with C3G siRNA #2 or control RNA and cultured for 2 d. Then cells were transfected with FLAG-siRNA-resistant C3G. The total cell lysates were subjected to SDS-PAGE, followed by immunoblotting with the anti-C3G pAb. (Cb) Neurite outgrowth in rescued PC12 cells. PC12 cells were cotransfected with pSUPER-retro-C3G and pERed NLS-FLAG vector (C3G-KD) or pERed NLS-FLAG siRNA-resistant C3G (C3G-rescue). Left panel: representative DIC images. Right panel: percentage of cells with neurites. (D) Effect of the double knockdown of C3G and PDZ-GEF1 on neurite outgrowth. PC12 cells were transfected with control siRNA (Control), PDZ-GEF1 siRNA #1 (PDZ-GEF-KD), C3G siRNA #1(C3G-KD), or PDZ-GEF1 siRNA #1 and C3G siRNA #1 (PDZ-GEF-KD, C3G-KD). Top panels: representative DIC images. Bottom panels: percentage of cells with neurites and the length of neurite. (E) Efficiency of the knockdown of Rap1 by three different siRNAs. PC12 cells were transfected with control siRNA (Cont) or Rap1 siRNAs #1-3. The immunoblot bands were quantified in the right panel. (F) Inhibition of neurite outgrowth in the Rap1-knockdown PC12 cells. PC12 cells were transfected with control siRNA (Control) or Rap1 siRNA #1-3 (Rap1-KD). Left panels: representative DIC images. Right panels: percentage of cells with neurites and the length of neurite. Asterisks indicate statistical significance (t test; *, $P < 0.01$). Bars, 10 μm.
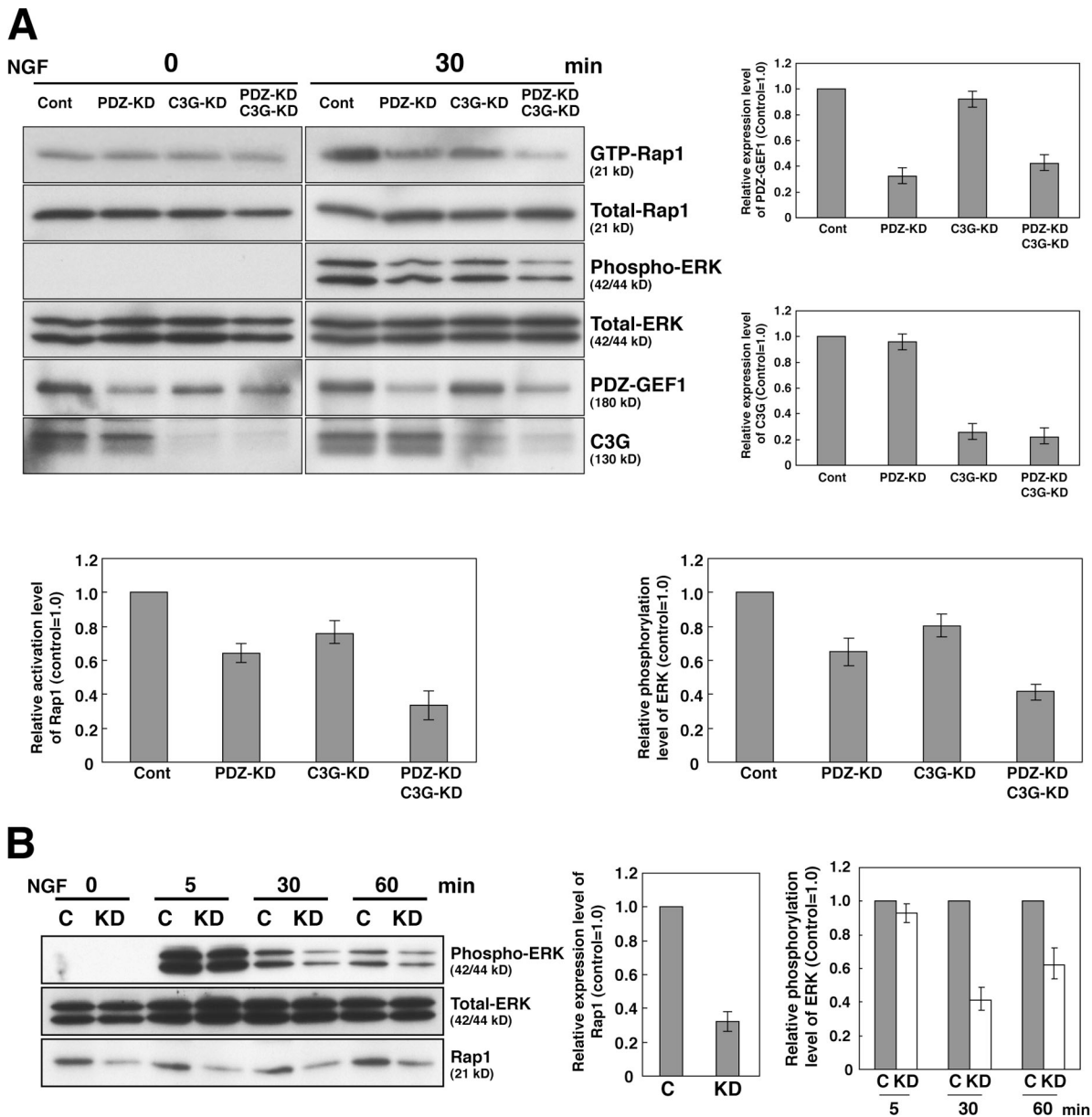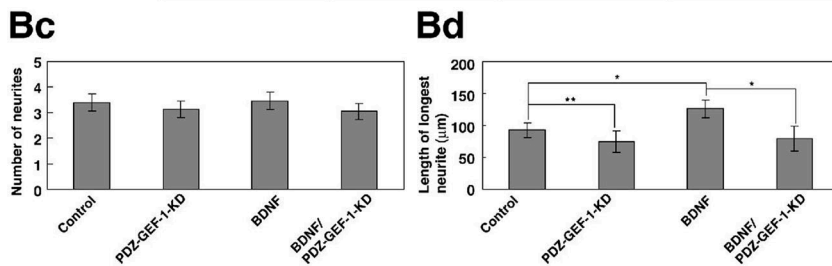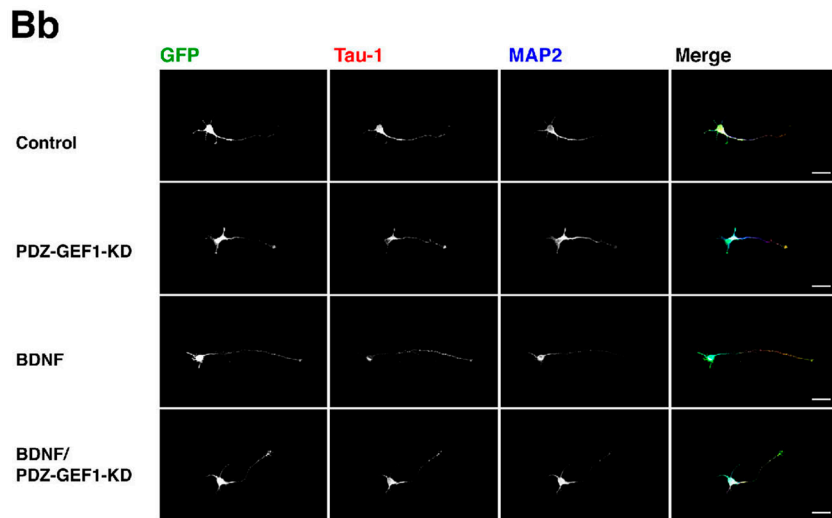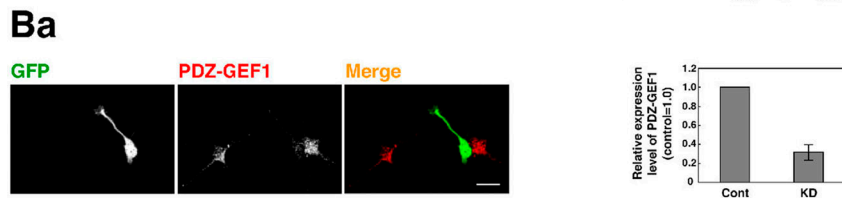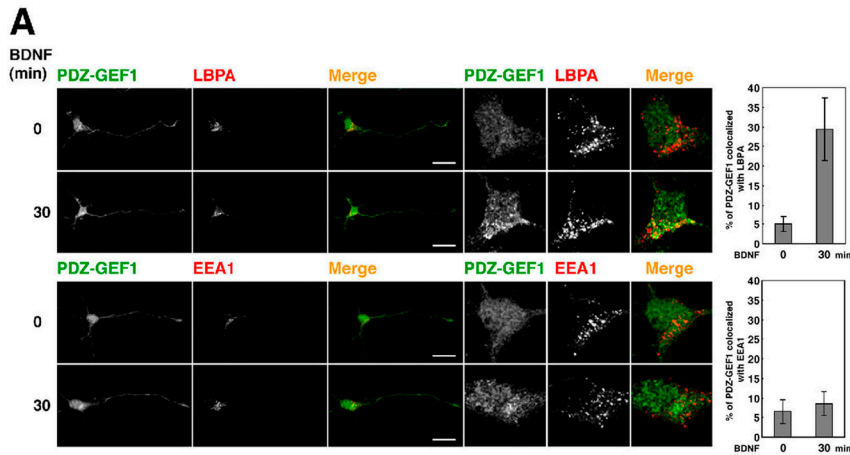
Figure 9. **Involvement of C3G and PDZ-GEF1 in the NGF-induced activation of Rap1 and ERK.** (A) Effects of the double knockdown of C3G and PDZ-GEF1 on the activation of Rap1 and ERK at 30 min after NGF stimulation in PC12 cells. PC12 cells were transfected with control RNA (Cont), PDZ-GEF1 siRNA #1 (PDZ-KD), C3G siRNA #1 (C3G-KD), or PDZ-GEF1 siRNA #1 and C3G siRNA #1 (PDZ-KD, C3G-KD). The pull-down assay was performed as described in Fig. 2 A. The immunoblot bands were quantified in the right and bottom panels. (B) The level of the activation of ERK in Rap1-knockdown PC12 cells. PC12 cells were transfected with control RNA (C) or Rap1 siRNA #1 (KD). The level of the activation of ERK was measured as described in Fig. 2 A. The immunoblot bands were quantified in the right panel.

The inhibitory effect of the knockdown of C3G on the NGF-induced sustained activation of Rap1 was less effective than that of the knockdown of PDZ-GEF1 (Fig. 9 A). The knockdown of PDZ-GEF1 alone did not completely abolish the NGF-induced sustained activation of Rap1. The double knockdown of C3G and PDZ-GEF1 more potently abolished the NGF-induced sustained activation of Rap1 and ERK. The inhibitory effect of the double knockdown of C3G and PDZ-GEF1 on the sustained activation of ERK was similar to that of the knockdown of Rap1 (Fig. 9, A and B). These results indicate that C3G and PDZ-GEF1 work cooperatively in the NGF-induced sustained activation of Rap1.

Involvement of PDZ-GEF1 in the BDNF-induced neurite outgrowth of hippocampal neurons

To validate the role of PDZ-GEF1 in PC12 cells, we finally examined whether PDZ-GEF1 is involved in the BDNF-induced neurite outgrowth in rat primary cultured hippocampal neurons. It has been reported that BDNF, but not NGF, enhances axon elongation in hippocampal neurons (Ip et al., 1993; Morfini et al., 1994; Labelle and Leclerc, 2000; Yoshimura et al., 2005). BDNF binds to its receptor, TrkB receptor, in hippocampal neurons (Huang and Reichardt 2001; Sofroniew et al., 2001). Retrograde transport of BDNF-TrkB and the signaling complex associating with it is

Figure 10. **Involvement of PDZ-GEF1 in the BDNF-induced neurite outgrowth in hippocampal neurons.** (A) Localization of endogenous PDZ-GEF1 at late endosomes in hippocampal neurons. Hippocampal neurons at 2.0 days in vitro were stimulated by BDNF for 30 min in the absence of serum and stained with indicated Abs. Insets are enlarged images of cell bodies. The area of colocalization was quantified in the right panel. Bars, 20 μm. (B) Inhibition of axon outgrowth in the PDZ-GEF1-knockdown hippocampal neurons. (Ba) Expression level of PDZ-GEF1 in knockdown neurons. Hippocampal neurons from E18 rats were cotransfected with GFP as a morphological marker along with pSUPER-retro-PDZ-GEF1 (PDZ-GEF1-KD) by electroporation. Transfected neurons were cultured for 1.5 d in the presence of BDNF, and allowed to extend axons and minor neurites. Transfected neurons were visualized by the GFP fluorescence (green) and immunostained with the anti-PDZ-GEF1 pAb (red). The fluorescence intensity of PDZ-GEF1 of the neurons expressing GFP was compared with that of the untransfected neurons in the same field of view in the right panel. (Bb) Effect of the knockdown of PDZ-GEF1 on axon outgrowth. The morphology of transfected neurons was visualized by the GFP fluorescence (green) and immunostained with the anti-Tau-1 mAb (red) and the anti-MAP2 pAb (blue). Bars, 20 μm. (Bc) Quantitative analysis of the number of neurite per transfected neuron. An average neurite number (± SEM) of between 40 and 60 analyzed neurons. (Bd) Quantitative analysis of the length of axon per transfected neuron. An average axon length (± SEM) of between 40 and 60 analyzed neurons. The mean value (± SEM) of three independent experiments is shown. Asterisks indicate statistical significance (t test; *, $P < 0.01$; **, $P < 0.05$). The results shown are representative of three independent experiments.

involved in the axon elongation and cell survival signal (Howe and Mobley, 2004; Zweifel et al., 2005). Hippocampal neurons at 2.0 days in vitro were stimulated by BDNF for indicated periods of time. PDZ-GEF1 was recruited to LBPA-positive late endosomes at 30 min after BDNF stimulation (Fig. 10 A). PDZ-GEF1 was not recruited to EEA1-positive early endosomes. Hippocampal neurons were cotransfected with an expression vector for GFP as a morphological marker along with the PDZ-GEF1 siRNA expression vector. At 1.5 days in vitro after plating, BDNF-induced recruitment of endogenous PDZ-GEF1 to late endosomes was not observed in the PDZ-GEF1-knockdown neurons (Fig. 10 Ba). The length of axon in the PDZ-GEF1-knockdown neurons was less than those of the control neurons (Fig. 10 B, b, c, and d). These results indicate that PDZ-GEF1 is involved in the BDNF-induced axon outgrowth in rat primary cultured hippocampal neurons.

Discussion

We first showed here that NGF induced the sustained activation of Rap1 at late endosomes and neurite outgrowth in cultured

PC12 cells. The activation of Rap1 at late endosomes was catalyzed by PDZ-GEF1. Earlier FRET studied showed that Rap1 was activated at peri-nuclear regions and it was practically difficult to distinguish the sites of the activation of Rap1 at the plasma membrane, early endosomes, and late endosomes by this method (Mochizuki et al., 2001; Ohba et al., 2003). We could not directly show the activation of Rap1 at late endosomes but indirectly showed it by immunofluorescence microscopy and immunoisolation analysis: PDZ-GEF1 was recruited to late endosomes in response to NGF. PDZ-GEF1 was not recruited to early endosomes, whereas C3G was recruited to early endosomes, but not to late endosomes. Thus, these two GEFs for Rap1 play roles in different compartments.

As Rap1 is first activated by C3G at the plasma membrane and early endosomes after NGF stimulation (Kao et al., 2001; Wu et al., 2001), activated Rap1 may affect the GEF activity of PDZ-GEF1. We found that the inhibitory effect of the knockdown of C3G on the NGF-induced sustained activation of Rap1 and neurite outgrowth was less effective than that of the knockdown of PDZ-GEF1. The knockdown of PDZ-GEF1 alone did not completely abolish the NGF-induced sustained activation of Rap1 or neurite outgrowth. The double knockdown of C3G and PDZ-GEF1 completely abolished the NGF-induced sustained activation of Rap1 and neurite outgrowth similar to the knockdown of Rap1. Thus, C3G and PDZ-GEF1 seem to work cooperatively in the NGF-induced sustained activation of Rap1 and neurite outgrowth. We found that C3G was recruited to early endosomes, but not to late endosomes. The activation of Rap1 was observed on late endosomes, not on early endosomes, at 30 min after NGF stimulation. Moreover, inhibition of the transport of TrkA receptor form early to late endosomes reduced the activation of Rap1 at 30 min after NGF stimulation. Collectively, we propose the following model for the activation of Rap1 by C3G and PDZ- GEF: (1) Upon NGF stimulation, C3G first activates Rap1 on early endosomes; (2) GTP-Rap1 on early endosomes is transported to late endosomes with TrkA receptor; and (3) Transported GTP-Rap1 activates PDZ-GEF1 and induces the sustained activation of Rap1 on late endosomes, eventually inducing neurite outgrowth.

The long-distance retrograde NGF signaling from axon terminals to cell bodies is crucial for neuronal survival and plasticity (Howe and Mobley 2004; Zweifel et al., 2005). It was shown that the internalization and endosomal trafficking of TrkA receptor are important for the long-distance retrograde NGF signaling (York et al., 2000; Ginty and Segal, 2002; Howe and Mobley, 2004). TrkA receptor continues to transduce a signal after its internalization into endosomes (York et al., 2000; Ginty and Segal, 2002; Howe and Mobley, 2004). Certain specialized endosomal organelles might represent signaling platforms from which specific pathways emerge (Howe et al., 2001; Sorkin and Von Zastrow, 2002). Earlier studies demonstrated that late endosomes are the major endosomal population labeled by endocytosed iodinated NGF in cell bodies of sympathetic neurons (Claude et al., 1982). As the interaction of TrkA receptor and NGF is resistant to decreasing pH values within the endosomal pathway (Zapf-Colby and Olefsky, 1998), it appears likely that NGF is still bound to the extracellular domain of TrkA receptor within late endosomes. Accordingly, immuno-electron microscopic study found phospho-TrkA receptor (pTrkA) immunoreactivity in late endosomes of sciatic-nerves (Bhattacharyya et al., 2002) and biochemical study found pTrkA in late endosomes in PC12 cells (Saxena et al., 2005a). Rab7, a member of the Rab family small G proteins, which regulates TrkA receptor transport from late endosomes to lysosomes, was shown to regulate the persistence of TrkA receptor at late endosomes and TrkA receptor signaling (Saxena et al., 2005b). Consistent with these earlier observations, we showed here by use of bafilomycin, an agent which inhibits the vesicular traffic from early endosomes to late endosomes, that the NGF-induced internalization and transport of TrkA receptor to late endosomes was essential for the sustained activation of Rap1 at late endosomes, the activation of ERK, and neurite outgrowth. Collectively with our findings, like TrkA receptor in clathrin-coated vesicles (Howe et al., 2001) and early endosomes (Delcroix et al., 2003), TrkA receptor in late endosomes is competent of signaling. In addition, there are several reports that receptor tyrosine kinases (RTKs) induce signaling from late endosomes. For instance, it is known that late endosomes contain phospho-EGF receptor (pEGFR and its activated downstream signaling components (Oksvold et al., 2001). The MAPK scaffold p14 localizes to the outer limiting membrane of late endosomes, and this localization is essential for EGFR signaling (Wunderlich et al., 2001). There is also in vivo evidence pointing toward the importance of late endosomes in the regulation of neuronal TGF-β signaling (Sweeney and Davis, 2002). Thus, late endosomes appear to be ideally suited for regulating spatial and temporal compartmentalization of signal transduction, beyond its conventional role in cargo degradation. Our report is the first to demonstrate that late endosomes represent functional TrkA receptor signaling platforms. This system might play a role in continuing activation state of NGF signaling during transport of TrkA receptor from axon terminals to cell bodies.

We furthermore showed here that PDZ-GEF1 was recruited to late endosomes to form a complex with TrkA receptor, which was internalized and transported there, and that recruited PDZ-GEF1 induced sustained activation of Rap1 and ERK. NGF-bound TrkA receptor activates its own tyrosine kinase and gathers the signaling complex consisting of C3G, CrkL, and FRS2 on the plasma membrane (Kao et al., 2001; Wu et al., 2001). TrkA receptor and the FRS2-Crk-C3G complex associating with the receptor are internalized into clathrin-coated vesicles and move into early endosomes within 5 min (Kao et al., 2001). Rap1 is activated at early endosomes and activated Rap1 induces the activation of the MAPK cascade through activating B-Raf (Wu et al., 2001). TrkA receptor then passes through early endosomes without entering into the recycling pathway to the plasma membrane and reaches to late endosomes within 30 min. Like the activated TrkA receptor complex at early endosomes, the TrkA receptor complex containing ARMS, S-SCAM, and PDZ-GEF1 at late endosomes was competent in activation of Rap1. While the GEF activity of C3G is activated by its interacting partner Crk (York et al., 1998), it remains unknown how the activity of PDZ-GEF1 is regulated at late endosomes. PDZ-GEF1 binds to the PDZ1

domain of S-SCAM through its C-terminal PDZ-binding motif and forms a stable complex (Ohtsuka et al., 1999). However, the binding of S-SCAM to PDZ-GEF1 does not affect GEF activity in vitro (Ohtsuka et al., 1999). The complex was recruited to ARMS-positive late endosomes through directly binding to ARMS, in a manner dependent on transport of TrkA receptor. The C-terminal PDZ-binding motif of PDZ-GEF1 contributed to direct the subcellular localization of PDZ-GEF1, leading to the augmented activation of Rap1 at late endosomes. Collectively, PDZ-GEF1 is recruited to late endosomes through its C-terminal PDZ-binding motif. PDZ-GEF1 then activates Rap1 at late endosomes and the GEF activity of PDZ-GEF1 is augmented by a positive feedback mechanism, resulting in the sustained activation of Rap1 at late endosomes. It may be noted that when TrkA receptor is transported from early endosomes to late endosomes, the FRS2-Crk-C3G complex associating with TrkA receptor remains at early endosomes, suggesting that this complex is dissociated from the receptor. The mechanism of this dissociation remains unknown and is an issue to be addressed in the future.

We finally showed here that the PDZ-GEF1-induced sustained activation of Rap1 at late endosomes was involved in the NGF-induced neurite outgrowth in PC12 cells and the BDNF-induced axon outgrowth in rat hippocampal neurons. What is the target protein(s) of Rap1 in the neurite outgrowth? Many downstream targets of Rap1 have been identified: they include c-Raf, B-Raf, RalGDS, afadin/AF-6, PI3-kinase, and RAPL (Bos et al., 2001; Kinashi and Katagiri, 2004; Nakanishi and Takai, 2004; Price and Bos, 2004). c-Raf and B-Raf are protein kinases connecting Ras to ERK; RalGDS is a regulator of another small G protein Ral; afadin/AF-6 is an actin filament- and nectin-binding protein at adherens junctions; PI3-kinase is a phosphatidylinositol kinase, and RAPL is a small protein which transduces a signal from Rap1 to integrin. Among them, for activating MAP kinase cascade, B-Raf was shown to be the target protein of Rap1 for the NGF-induced neurite outgrowth (Ohtsuka et al., 1996). Several transcription factors, which are downstream of the MAP kinase cascade, contribute to neurite outgrowth by gene expression. On the other hand, RAPL and its binding protein Mst1 were recently shown to be involved in transport of integrin LFA-1 and its activation in lymphocytes (Katagiri et al., 2006). Transport of transmembrane proteins from late endosomes to the plasma membrane is an emerging paradigm and generally accepted (Mellman and Steinman, 2001; Trajkovic et al., 2006; van Niel et al., 2006). Accordingly, activation of Rap1 at late endosomes might be involved in the transport of integrin from late endosomes to the plasma membrane and thereby regulate the activation of MAP kinase cascade indirectly. Moreover, we previously identified RA-RhoGAP as another direct downstream target of Rap1 (Yamada et al., 2005). RA-RhoGAP has the RA and GAP domains in addition to the PH and annexin-like repeat domains. It indeed shows a GAP activity specific for Rho and this GAP activity is enhanced by GTP-Rap1. The Rap1-RA-RhoGAP-Rho pathway plays an important role in the neurite outgrowth. Collectively, during the initiation of the neurite outgrowth, a neurite formation signal(s), such as NGF and BDNF, induces the C3G-mediated activation

of Rap1 at endocytic vesicles or early endosomes in a growth cone of the nascent neurite. Subsequently, RA-RhoGAP is recruited and activated by Rap1 to cause the inactivation of Rho at the growth cone of the nascent neurite. Repression of the Rho-mediated signaling pathway induces rapid actin depolymerization of the growth cone and thereby extends the incipient neurite further. In addition, to replenish the requirement for neurite outgrowth, such as signaling molecules and cytoskeletal proteins, endocytic vesicles or early endosomes are transported to late endosomes to sustain the activation of Rap1 by PDZ-GEF1. The sustained activation of Rap1 prolongs the activation time of the MAPK cascade and results in the up-regulation of gene expression. Thus, the Rap1-RA-RhoGAP-Rho system and the PDZ-GEF-Rap1-B-Raf-MAPK system could cooperatively regulate neurite outgrowth. In future studies, it will be important to elucidate how these two systems are spatially and temporally activated during the neurite outgrowth.

Materials and methods

Expression vectors

pFLAG-CMV2-PDZ-GEF1 and pFLAG-CMV2-PDZ-GEF1-ΔRA were obtained from Dr. Tohru Kataoka (Kobe University, Kobe, Japan). The RNAi-resistant mutant of FLAG-human PDZ-GEF1 (pERedNLS-FLAG-PDZ-GEF1^R) was generated by mutagenesis of 5′-GAGAGATTGTTATGGTGAA-3′ to 5′-GCGAA-ATCGTTATGGTTAA-3′ using the QuikChange site-directed mutagenesis kit (Stratagene). The letters in the codons, which are different from the letters in the RNAi sequence of rat PDZ-GEF1, are underlined. pCMV-HA-PDZ-GEF1 was constructed using standard molecular biology methods. pCI-neo-Myc-S-SCAM, pCIneo-Myc-S-SCAM-8, pCIneo-Myc-S-SCAM-10, and pCIneo-Myc-S-SCAM-12 were obtained from Dr. Yutaka Hata (Tokyo Medical and Dental University, Tokyo, Japan). pCIneo-Myc-S-SCAM-ΔPDZ4 (aa 929–1010 deletion) was constructed using standard molecular biology methods. KIAA1250/ARMS cDNA was obtained from Dr. Takahiro Nagase (Kazusa DNA Research Institute, Chiba, Japan). pCMV-FLAG-ARMS, pGEX4T-2-ARMS-Ct (aa 1616–1715), and pGEX4T-2-ARMS-Ct-ΔSIl (aa 1616–1712) were constructed using standard molecular biology methods. pCMV-FLAG-C3G was constructed using standard molecular biology methods. The RNAi-resistant mutant of FLAG-human C3G (pERedNLS-FLAG-C3G^R) was generated by mutagenesis of 5′-GCTCCTCATGGAGGTATAC -3′ to 5′-GCTCCTCATGGAAGTATAC-3′ using the QuikChange site-directed mutagenesis kit (Stratagene). The letters in the codons, which are different from the letters in the RNAi sequence of rat C3G, are underlined. pGEX4T-1-RalGDS-3xRBD was constructed using standard molecular biology methods.

Antibodies

The GST-fusion fragment of PDZ-GEF1 (aa 1–250) was produced in *Escherichia coli*, purified, and used as an antigen to raise a pAb in rabbit. The rabbit anti-PDZ-GEF1 pAb was affinity purified by using MBP-PDZ-GEF1 (aa 1–250) immobilized on Amino-link agarose beads (Pierce Chemical Co). A rabbit anti-S-SCAM pAb was obtained from Dr. Yutaka Hata (Tokyo Medical and Dental University, Tokyo, Japan). A mouse anti-LBPA mAb was obtained from Dr. Toshihide Kobayashi (RIKEN, Wako, Japan) and Dr. Jean Gruenberg (University of Geneva, Geneva, Switzerland). A rabbit anti-Rab7 pAb was obtained from Dr. Marino Zerial (Max Plank Institute, Dresden, Germany). A rabbit anti-Rap1 pAb, a mouse anti-pan-Trk mAb (B-39), a rabbit anti-C3G pAb, a mouse anti-cMyc mAb (9E10), and a mouse anti-GST mAb (B-14) were purchased from Santa Cruz Biotechnology, Inc. A mouse anti-phospho-ERK mAb (E10) and a rabbit anti-ERK pAb were purchased from Cell Signaling. A mouse anti-Ras mAb and a rabbit anti-TrkA receptor pAb were purchased from Upstate Biotechnology. A mouse anti-EEA1 mAb and a mouse anti-GM130 mAb were purchased from Transduction Laboratories. A mouse anti-FLAG M2 mAb and a rabbit anti-FLAG pAb were purchased from Sigma-Aldrich. A mouse anti-Kidins220/ARMS mAb was purchased from Abcam. A rabbit anti-Kidins220/ARMS pAb was purchased from ABR. A mouse anti-Tau-1 mAb and a rabbit anti-MAP2 pAb were purchased from Chemicon International. A mouse anti-HA mAb was purchased from Babco.

Knockdown of PDZ-GEF1, ARMS, and C3G by the RNAi method

For PDZ-GEF1-knockdown, double-stranded 19-nucleotide RNA duplexes (QIAGEN) for PDZ-GEF1 #1 (5′-GAGAGAUUGUAAUGGUGAA-3′), #2 (5′-GAGUAGAGAGAGAGUCUUGAA-3′), scramble RNA for #1 (5′-AAU-UGUAAUAGGAUGGGAG-3′), or double-stranded 25-nucleotide RNA duplexes (StealthTM RNA-mediated interference; Invitrogen) for PDZ-GEF1 #3 (5′-CGAUCCAGUAUUGUCAGCAAUUCUU-3′) was transfected into PC12 cells using Lipofectamine 2000 reagent. For C3G-knockdown, double-stranded 25-nucleotide RNA duplexes (Stealth RNA-mediated interference; Invitrogen) for C3G #1 (5′-CAGAACGAGAAAUGGAGAUUC-UGAA-3′), double-stranded 19-nucleotide RNA duplexes (QIAGEN) for C3G #2 (5′-GAUGCUCAUGGAGGUCUAU-3′), #3 (5′-CCAGACUAC-AUAGACGGGAAGGUCA-3′), or scramble RNA for #1 (5′-AGAGUUA-GCGGCGAAUAUAAAAAGC-3′) was transfected into PC12 cells using Lipofectamine 2000 reagent. For ARMS-knockdown, double-stranded 25-nucleotide RNA duplexes (StealthTM RNA-mediated interference; Invitrogen) for ARMS #1 (5′-CAGGCCGAGUAUAGAGACGCCUAUA-3′), #2 (5′-CGGCUCUCAACAGAAGGGACACUUA-3′), #3 (5′-GGGCUCCAU-CCAUUCUACUCUAGAA-3′), or scramble RNA for #1 (5′-CAGGAGC-AUAUAGAGCCGCUCGAUA-3′) was transfected into PC12 cells using Lipofectamine 2000 reagent. For Rap1-knockdown, double-stranded 25-nucleotide RNA duplexes (StealthTM RNA-mediated interference; Invitrogen) for Rap1 #1 (5′-CAGAAUUUAGCAAGACAGUGGUGUA-3′), #2 (5′-CAGCAAUGAGGGAUUUGUAUAUGAA-3′), or #3 (5′-UGGGAAA-GUCUGCUCUGACAGUUCA-3′) was transfected into PC12 cells using Lipofectamine 2000 reagent. For detection of knockdown efficiency, the whole cell lysates of PC12 cells were subjected to SDS-PAGE, followed by immunoblotting with the anti-PDZ-GEF1 pAb, the anti-C3G pAb, the anti-ARMS pAb, or the anti-actin mAb. For FRET analysis and rescue experiment in neurite outgrowth, the siRNA expression vector, pSUPER-retro was used for expression of shRNA in PC12 cells. The following inserts were used: PDZ-GEF1 gene-specific insert was a 19-nucleotide sequence corresponding to nucleotides 740–758 (5′-GAGAGAUUGUAAUGGUGAA-3′) of PDZ-GEF1 cDNA, which was separated by a 10-nucleotide noncomplementary spacer (TTCAAGAGA) from the reverse complement of the same 19-nucleotide sequence. C3G gene-specific insert was a 19-nucleotide sequence corresponding to nucleotides 1407–1425 (5′-GATGCTCATGG-AGGTCTAT-3′) of C3G cDNA, which was separated by a 10-nucleotide noncomplementary spacer (TTCAAGAGA) from the reverse complement of the same 19-nucleotide sequence.

Rap1 GEF assay

GEF assay was performed as described previously (Yamamoto et al., 1990). Lipid-modified GST-Rap1A was generated in Sf9 cells using the baculovirus expression system as described previously (Mizuno et al., 1991; Umikawa et al., 1999). FLAG-PDZ-GEF1 and FLAG-PDZ-GEF1-ΔRA were purified from transfected HEK 293 cells as described previously (Kimura et al., 2006). Lipid-modified GDP-bound form of GST-Rap1A (5 pmol) was incubated at 30°C for indicated periods of time in a reaction mixture (50 μl) containing FLAG-PDZ-GEF1 (0.5 pmol) with or without the GST-Rap1A-CA (5 pmol), 50 mM Tris/HCl at pH 8.0, 12 mM MgCl$_2$, 2 mM EDTA, 0.4 mM DTT, 0.06% CHAPS, and 12 μM [^{35}S]GTPγS (6×10^3 cpm/pmol). The mixture was applied to a nitrocellulose filter, and the radioactivity retained on the filter was measured.

FRET imaging

PC12 cells were transfected with an empty pSUPER-retro vector or pSUPER-retro-PDZ-GEF1. After selection with puromycin, cells were further transfected with pRaichu-Rap1. PC12 cells expressing Raichu-Rap1 were starved for 6–12 h with phenol red-free DMEM/F12 medium containing 0.1% bovine serum albumin (BSA), and then treated with 50 ng/ml of NGF. The medium was covered with mineral oil (Sigma-Aldrich) to preclude evaporation. Cells were imaged with an IX71 inverted microscope (Olympus) equipped with a Cool SNAP-HQ cooled CCD camera (Roper Scientific) controlled with MetaMorph software (Universal Imaging), as described previously (Mochizuki et al., 2001). The filters used for the dual-emission imaging studies were obtained from Omega Optical: an XF1071 (440AF21) excitation filter, an XF2034 (455DRLP) dichroic mirror, and two emission filters (XF3075 (480AF30) for CFP and XF3079 (535AF26) for YFP). Cells were illuminated with a 75-W Xenon lamp through a 12% ND filter and viewed through a 60x immersion objective lens. The exposure times for 4×4 binning were 400 msec for CFP and YFP images, and 100 msec for differential interference contrast (DIC) images. After background subtraction, YFP/CFP ratio images were created with the MetaMorph software and the images were used to represent FRET efficiency.

Immunofluorescence and confocal microscopy

Staining was performed as follows: PC12 cells were seeded onto poly-L-lysine coated coverslips in 24-well plates a day before the experiment. PC12 cells were cultured in DME with serum for 24 h, serum-starved for 16 h, treated with bafilomycin for 2 h, and stimulated by NGF for 30 min. The cells were fixed with 4% paraformaldehyde for 15 min and permeabilized with 0.05% Saponin for 30 min at room temperature. Images were captured using a Carl Zeiss confocal laser scanning microscope using a 63× oil immersion objective lens (model LSM 510-V3.2; Carl Zeiss MicroImaging, Inc.) or a confocal laser scanning microscope (model TE2000; Nikon) using a 60× oil immersion objective lens. The fluorescence area and intensity of each protein in PC12 cells were measured by use of NIH Image software. Collected data were exported as 8-bit TIFF files and processed using Adobe Photoshop 7.0.

Pull-down assay for GTP-Rap1 and GTP-Ras

The pull-down assay was performed as described previously (Sasagawa et al., 2005). PC12 cells were transfected with siRNA for 2 d and stimulated by NGF for indicated periods of time. The PC12 cells were washed with 1 ml of ice-cold PBS and lysed in Buffer A (50 mM Tris/HCl at pH 7.4, 150 mM NaCl, 5 mM MgCl$_2$, 1% NP-40, 0.5% sodium deoxycholate, 0.1% SDS, 1 mM phenylmethylsulfonyl fluoride, 1 mM sodium vanadate). The samples were centrifuged at 100,000 x g for 10 min, and the supernatant was collected as the cell lysates. For the Rap1 pull down assay, the cell lysate (600 μg of protein) was incubated with GST-RalGDS Rap binding domain (RBD) (10 μg of protein) immobilized on glutathione-Sepharose beads (50 μl) for 30 min. After the beads were washed three times with Buffer A, GTP-Rap1 was detected by immunoblotting with an anti-Rap1 pAb. For the Ras pull-down assay, the cell lysate (600 μg of protein) was incubated with GST-c-Raf Ras binding domain (RBD) (30 μg of protein) immobilized on glutathione-Sepharose beads (50 μl) for 30 min. After the beads were washed three times with Buffer A, GTP-Ras was detected by immunoblotting with an anti-Ras mAb.

Detection of ERK activation

5% of the total cell lysates of PC12 cells was used for immunoblotting with either the anti-phospho-ERK mAb or the anti-ERK pAb to determine the amount of activated ERK (Phospho-ERK) or the total amount of ERK (Total-ERK), respectively, in each transfected cells.

Quantification of neurites

PC12 cells were obtained from Dr. Shinya Kuroda (Tokyo University, Tokyo, Japan) and maintained in DMEM with 5% horse serum and 10% bovine calf serum (Hyclone) in a 10% CO$_2$ atmosphere. PC12 cells were cultured in DMEM with serum for 48 h and stimulated by NGF for 24 h. Images were captured using a confocal laser scanning microscope using a 60× oil immersion objective lens (model TE2000; Nikon). Collected data were exported as 8-bit TIFF files and processed using Adobe Photoshop software. The assay for neurite outgrowth was performed on 40–60 cells randomly chosen in each group. The number of primary neurites per cell was defined as the number of thin cell processes with a length longer than one cell diameter. The statistical significance of differences between each group was analyzed by the two-tailed t test.

Rat hippocampal neurons were prepared form embryonic day (E) 18 Sprague-Dawley rats with slight modifications as described (Goslin and Banker, 1989). For cDNA transfection, before plating, the cells were resuspended in an optimized transfection solution for primary rat hippocampal neurons (Amaxa). Each sample (2×10^6 cells in 100 μl) was transfected with 2 μg cDNA as indicated by using Nucleofector electroporation device (Amaxa), according to the optimized protocol for primary rat hippocampal neurons (Amaxa). Immediately after transfection, the cells were cultured in 24-multiwells at a density of 3×10^4 cells/well. After 1.5 d culture, neurons were processed for immunohistochemistry. Images were captured using a confocal laser scanning microscope using 40 and 60× oil immersion objective lens (model TE2000; Nikon). Collected data were exported as 8-bit TIFF files and processed using Adobe Photoshop software. The morphometrical analysis for axons and minor neurites was performed on between 40 and 60 GFP-positive neurons (Ahnert-Hilger et al., 2004). The number of axons or minor neurites per cell was defined as the number of Tau-1-positive processes at least twice as long as the other processes or MAP2-positive processes longer than one cell diameter, respectively. The length of individual axons for each neuron was measured by use of the NIH Image software. Axon length encompasses all visible parts of an axon without the length of its branches. The statistical significance of differences between each group was analyzed by the two-tailed t test.

Subcellular fractionation

PC12 cells (cultured on 3 × 10 cm plates) were cracked with a ball-bearing homogenizer in Buffer B (250 mM sucrose, 3 mM imidazole at pH 7.4, 1 mM EDTA, 10 μg/ml cycloheximide, and complete protease inhibitor cocktail [Roche]). Subsequently, a post-nuclear supernatant (PNS) was prepared by centrifugation at 3000 rpm for 10 min (Kubota 5800). The PNS was adjusted to 40.6% sucrose, loaded at the bottom of a p55ST centrifuge tube (Hitachi), and overlaid sequentially with 35% and 30.5% sucrose solutions in 3 mM imidazole at pH 7.4, 1 mM EDTA, and 10 μg/ml cycloheximide. Subsequently, the tube was filled up with the homogenization buffer. The gradient was centrifuged at 35,000 rpm for 66 min using a p55ST rotor (Hitachi). After the centrifugation, the different interfaces and sucrose cushions were collected from top to bottom of the tube. Heavy membrane fraction was recovered in the 40.6/35% fraction. Early endosomal fraction was recovered in the 35/30.5% fraction. Late endosomal fraction was recovered in the 30.5/8% fraction. BCA assays (Pierce Chemical Co.) were performed to determine the protein concentration of each fraction. Equal amounts of protein from each fraction were loaded on SDS-PAGE, followed by immunoblotting with the mouse anti-GM130 mAb, the mouse anti-EEA1 mAb, the rabbit anti-Rab7 pAb, and the rabbit anti-Rap1 pAb.

For detecting GTP-Rap1, PC12 cells (cultured on 3 × 10 cm plates) were cracked with a ball-bearing homogenizer in Buffer C (250 mM sucrose, 3 mM imidazole at pH 7.4, 1 mM EDTA, 10 μg/ml cycloheximide, complete protease inhibitor cocktail [Roche], and 100 μg/ml GST-RalGDS-3xRBD). Subsequently, the PNS was prepared and used for the subcellular fractionation as described above. Equal amounts of protein from each fraction were loaded on SDS-PAGE, followed by immunoblotting with the mouse anti-GST mAb, the rabbit anti-Rap1 pAb, and the mouse anti-Ras mAb.

Immunoisolation of PDZ-GEF1–containing vesicles

Immunoisolation of vesicles was performed as described previously (Saucan and Palade, 1994). In brief, PC12 cells (cultured on 4 × 10 cm plates) were starved for 16 h in phenol red-free DMEM/F12 medium containing 0.1% BSA, and either left unstimulated or stimulated by NGF for 30 min. Subsequently, the cells were cracked with a ball-bearing homogenizer in Buffer B. Subsequently, a PNS was prepared by centrifugation at 3,000 rpm for 10 min (Kubota 5800). Dynabeads Protein A (DYNAL Inc.) magnetic beads were coated with the anti-PDZ-GEF1 pAb or the control IgG at a density of 10 μg Ab per 50 μl beads according to manufacturer's instructions. The anti-PDZ-GEF1 pAb-coated beads were added to the PNS and incubated with continuous rotation at 4°C for 2 h. The immunoisolated beads were washed five times with Buffer B using a magnet and transferred to fresh tubes. The beads were finally resuspended in 80 μl of the SDS sample buffer for SDS-PAGE, followed by immunoblotting with the mouse anti-EEA1 mAb, the rabbit anti-Rab7 pAb, the anti-ARMS mAb, and the rabbit anti-PDZ-GEF1.

Online supplemental material

Fig. S1 shows the effect of GTP-Rap1 on the GEF activity of PDZ-GEF1-ΔRA. Fig. S2 shows the effect of overexpression of PDZ-GEF1 on neurite outgrowth. Fig. S3 shows the recruitment of C3G to early endosomes in a NGF-dependent manner. Fig. S4 shows the Inhibition of the transport of TrkA receptor from early endosomes to late endosomes by bafilomycin. Fig. S5 shows the expression levels of S-SCAM and ARMS in S-SCAM-expressing- and ARMS-knockdown PC12 cells, respectively. Online supplemental material is available at http://www.jcb.org/cgi/content/full/jcb.200610073/DC1.

References

Ahnert-Hilger, G., M. Holtje, G. Grosse, G. Pickert, C. Mucke, B. Nixdorf-Bergweiler, P. Boquet, F. Hofmann, and I. Just. 2004. Differential effects of Rho GTPases on axonal and dendritic development in hippocampal neurons. *J. Neurochem.* 90:9–18.

Arevalo, J.C., H. Yano, K.K. Teng, and M.V. Chao. 2004. A unique pathway for sustained neurotrophin signaling through an ankyrin-rich membrane-spanning protein. *EMBO J.* 23:2358–2368.

Arevalo, J.C., D.B. Pereira, H. Yano, K.K. Teng, and M.V. Chao. 2006. Identification of a switch in neurotrophin signaling by selective tyrosine phosphorylation. *J. Biol. Chem.* 281:1001–1007.

Beranger, F., B. Goud, A. Tavitian, and J. de Gunzburg. 1991. Association of the Ras-antagonistic Rap1/Krev-1 proteins with the Golgi complex. *Proc. Natl. Acad. Sci. USA.* 88:1606–1610.

Bhattacharyya, A., F.L. Watson, S.L. Pomeroy, Y.Z. Zhang, C.D. Stiles, and R.A. Segal. 2002. High-resolution imaging demonstrates dynein-based vesicular transport of activated Trk receptors. *J. Neurobiol.* 51:302–312.

Bito, H., T. Furuyashiki, H. Ishihara, Y. Shibasaki, K. Ohashi, K. Mizuno, M. Maekawa, T. Ishizaki, and S. Narumiya. 2000. A critical role for a Rho-associated kinase, p160ROCK, in determining axon outgrowth in mammalian CNS neurons. *Neuron.* 26:431–441.

Bos, J.L., J. de Rooij, and K.A. Reedquist. 2001. Rap1 signalling: adhering to new models. *Nat. Rev. Mol. Cell Biol.* 2:369–377.

Claude, P., E. Hawrot, D.A. Dunis, and R.B. Campenot. 1982. Binding, internalization, and retrograde transport of ^{125}I-nerve growth factor in cultured rat sympathetic neurons. *J. Neurosci.* 2:431–442.

Craig, A.M., R.J. Wyborski, and G. Banker. 1995. Preferential addition of newly synthesized membrane protein at axonal growth cones. *Nature.* 375:592–594.

Da Silva, J.S., and C.G. Dotti. 2002. Breaking the neuronal sphere: regulation of the actin cytoskeleton in neuritogenesis. *Nat. Rev. Neurosci.* 3:694–704.

Da Silva, J.S., M. Medina, C. Zuliani, A. Di Nardo, W. Witke, and C.G. Dotti. 2003. RhoA/ROCK regulation of neuritogenesis via profilin IIa-mediated control of actin stability. *J. Cell Biol.* 162:1267–1279.

de Rooij, J., N.M. Boenink, M. van Triest, R.H. Cool, A. Wittinghofer, and J.L. Bos. 1999. PDZ-GEF1, a guanine nucleotide exchange factor specific for Rap1 and Rap2. *J. Biol. Chem.* 274:38125–38130.

Delcroix, J.D., J.S. Valletta, C. Wu, S.J. Hunt, A.S. Kowal, and W.C. Mobley. 2003. NGF signaling in sensory neurons: evidence that early endosomes carry NGF retrograde signals. *Neuron.* 39:69–84.

Ginty, D.D., and R.A. Segal. 2002. Retrograde neurotrophin signaling: Trk-ing along the axon. *Curr. Opin. Neurobiol.* 12:268–274.

Goslin, K., and G. Banker. 1989. Experimental observations on the development of polarity by hippocampal neurons in culture. *J. Cell Biol.* 108:1507–1516.

Herrmann, C., G. Horn, M. Spaargaren, and A. Wittinghofer. 1996. Differential interaction of the Ras family GTP-binding proteins H-Ras, Rap1A, and R-Ras with the putative effector molecules Raf kinase and Ral-guanine nucleotide exchange factor. *J. Biol. Chem.* 271:6794–6800.

Hirao, K., Y. Hata, N. Ide, M. Takeuchi, M. Irie, I. Yao, M. Deguchi, A. Toyoda, T.C. Sudhof, and Y. Takai. 1998. A novel multiple PDZ domain-containing molecule interacting with N-methyl-D-aspartate receptors and neuronal cell adhesion proteins. *J. Biol. Chem.* 273:21105–21110.

Horton, A.C., and M.D. Ehlers. 2003. Neuronal polarity and trafficking. *Neuron.* 40:277–295.

Howe, C.L., and W.C. Mobley. 2004. Signaling endosome hypothesis: A cellular mechanism for long distance communication. *J. Neurobiol.* 58:207–216.

Howe, C.L., J.S. Valletta, A.S. Rusnak, and W.C. Mobley. 2001. NGF signaling from clathrin-coated vesicles: evidence that signaling endosomes serve as a platform for the Ras-MAPK pathway. *Neuron.* 32:801–814.

Huang, E.J., and L.F. Reichardt. 2001. Neurotrophins: roles in neuronal development and function. *Annu. Rev. Neurosci.* 24:677–736.

Hurtado-Lorenzo, A., M. Skinner, J. El Annan, M. Futai, G.H. Sun-Wada, S. Bourgoin, J. Casanova, A. Wildeman, S. Bechoua, D.A. Ausiello, et al. 2006. V-ATPase interacts with ARNO and Arf6 in early endosomes and regulates the protein degradative pathway. *Nat. Cell Biol.* 8:124–136.

Ip, N.Y., Y. Li, G.D. Yancopoulos, and R.M. Lindsay. 1993. Cultured hippocampal neurons show responses to BDNF, NT-3, and NT-4, but not NGF. *J. Neurosci.* 13:3394–3405.

Jalink, K., T. Eichholtz, F.R. Postma, E.J. van Corven, and W.H. Moolenaar. 1993. Lysophosphatidic acid induces neuronal shape changes via a novel, receptor-mediated signaling pathway: similarity to thrombin action. *Cell Growth Differ.* 4:247–255.

Jullien, J., V. Guili, L.F. Reichardt, and B.B. Rudkin. 2002. Molecular kinetics of nerve growth factor receptor trafficking and activation. *J. Biol. Chem.* 277:38700–38708.

Kao, R. K. Jaiswal, W. Kolch, and G.E. Landreth. 2001. Identification of the mechanisms regulating the differential activation of the mapk cascade by epidermal growth factor and nerve growth factor in PC12 cells. *J. Biol. Chem.* 276:18169–18177.

Katagiri, K., M. Imamura, and T. Kinashi. 2006. Spatiotemporal regulation of the kinase Mst1 by binding protein RAPL is critical for lymphocyte polarity and adhesion. *Nat. Immunol.* 7:919–928.

Kimura, T., T. Sakisaka, T. Baba, T. Yamada, and Y. Takai. 2006. Involvement of the Ras-Ras-activated Rab5 guanine nucleotide exchange factor RIN2-Rab5

pathway in the hepatocyte growth factor-induced endocytosis of E-cadherin. *J. Biol. Chem.* 281:10598–10609.

Kinashi, T., and K. Katagiri. 2004. Regulation of lymphocyte adhesion and migration by the small GTPase Rap1 and its effector molecule, RAPL. *Immunol. Lett.* 93:1–5.

Kong, H., J. Boulter, J.L. Weber, C. Lai, and M.W. Chao. 2001. An evolutionarily conserved transmembrane protein that is a novel downstream target of neurotrophin and ephrin receptors. *J. Neurosci.* 21:176–185.

Kozma, R., S. Sarner, S. Ahmed, and L. Lim. 1997. Rho family GTPases and neuronal growth cone remodelling: relationship between increased complexity induced by Cdc42Hs, Rac1, and acetylcholine and collapse induced by RhoA and lysophosphatidic acid. *Mol. Cell. Biol.* 17:1201–1211.

Labelle, C., and N. Leclerc. 2000. Exogenous BDNF, NT-3 and NT-4 differentially regulate neurite outgrowth in cultured hippocampal neurons. *Brain Res. Dev. Brain Res.* 123:1–11.

Liao, Y., K. Kariya, C.D. Hu, M. Shibatohge, M. Goshima, T. Okada, Y. Watari, X. Gao, T.G. Jin, Y. Yamawaki-Kataoka, and T. Kataoka. 1999. RA-GEF, a novel Rap1A guanine nucleotide exchange factor containing a Ras/Rap1A-associating domain, is conserved between nematode and humans. *J. Biol. Chem.* 274:37815–37820.

Liao, Y., T. Satoh, X. Gao, T.G. Jin, C.D. Hu, and T. Kataoka. 2001. RA-GEF-1, a guanine nucleotide exchange factor for Rap1, is activated by translocation induced by association with Rap1-GTP and enhances Rap1-dependent B-Raf activation. *J. Biol. Chem.* 276:28478–28483.

Mellman, I., and R.M. Steinman. 2001. Dendritic cells: specialized and regulated antigen processing machines. *Cell.* 106:255–258.

Mitchison, T., and M. Kirschner. 1998. Cytoskeletal dynamics and nerve growth. *Neuron.* 1:761–772.

Mizuno, T., K. Kaibuchi, T. Yamamoto, M. Kawamura, T. Sakoda, H. Fujioka, Y. Matsuura, and Y. Takai. 1991. A stimulatory GDP/GTP exchange protein for smg p21 is active on the post-translationally processed form of c-Ki-ras p21 and rhoA p21. *Proc. Natl. Acad. Sci. USA.* 88:6442–6446.

Mochizuki, N., S. Yamashita, K. Kurokawa, Y. Ohba, T. Nagai, A. Miyawaki, and M. Matsuda. 2001. Spatio-temporal images of growth-factor-induced activation of Ras and Rap1. *Nature.* 411:1065–1068.

Morfini, G., M.C. DiTella, F. Feiguin, N. Carri, and A. Caceres. 1994. Neurotrophin-3 enhances neurite outgrowth in cultured hippocampal pyramidal neurons. *J. Neurosci. Res.* 39:219–232.

Nakanishi, H., and Y. Takai. 2004. Roles of nectins in cell adhesion, migration and polarization. *Biol. Chem.* 385:885–892.

Ohba, Y., K. Kurokawa, and M. Matsuda. 2003. Mechanism of the spatio-temporal regulation of Ras and Rap1. *EMBO J.* 22:859–869.

Ohtsuka, T., K. Shimizu, B. Yamamori, S. Kuroda, and Y. Takai. 1996. Activation of brain B-Raf protein kinase by Rap1B small GTP-binding protein. *J. Biol. Chem.* 271:1258–1261.

Ohtsuka, T., Y. Hata, N. Ide, T. Yasuda, E. Inoue, T. Inoue, A. Mizoguchi, and Y. Takai. 1999. nRap GEP: a novel neural GDP/GTP exchange protein for rap1 small G protein that interacts with synaptic scaffolding molecule (S-SCAM). *Biochem. Biophys. Res. Commun.* 265:38–44.

Oksvold, M.P., E. Skarpen, L. Wierod, R.E. Paulsen, and H.S. Huitfeldt. 2001. Re-localization of activated EGF receptor and its signal transducers to multivesicular compartments downstream of early endosomes in response to EGF. *Eur. J. Cell Biol.* 80:285–294.

Pizon, V., M. Desjardins, C. Bucci, R.G. Parton, and M. Zerial. 1994. Association of Rap1 and Rap1b proteins with late endocytic/phagocytic compartments and Rap2a with the Golgi complex. *J. Cell Sci.* 107:1661–1670.

Price, L.S., and J.L. Bos. 2004. RAPL: taking the Rap in immunity. *Nat. Immunol.* 5:1007–1008.

Sasagawa, S., Y. Ozaki, K. Fujita, and S. Kuroda. 2005. Prediction and validation of the distinct dynamics of transient and sustained ERK activation. *Nat. Cell Biol.* 7:365–373.

Saucan, L., and G.E. Palade. 1994. Membrane and secretory proteins are transported from the Golgi complex to the sinusoidal plasmalemma of hepatocytes by distinct vesicular carriers. *J. Cell Biol.* 125:733–741.

Saxena, S., C.L. Howe, J.M. Cosgaya, P. Steiner, H. Hirling, J.R. Chan, J. Weis, and A. Kruttgen. 2005a. Differential endocytic sorting of p75NTR and TrkA in response to NGF: a role for late endosomes in TrkA trafficking. *Mol. Cell. Neurosci.* 28:571–587.

Saxena, S., C. Bucci, J. Weis, and A. Kruttgen. 2005b. The small GTPase Rab7 controls the endosomal trafficking and neuritogenic signaling of the nerve growth factor receptor TrkA. *J. Neurosci.* 25:10930–10940.

Schwamborn, J.C., and A.W. Püschel. 2004. The sequential activity of the GTPases Rap1B and Cdc42 determines neuronal polarity. *Nat. Neurosci.* 7:923–929.

Snider, W.D. 1994. Functions of the neurotrophins during nervous system development: what the knockouts are teaching us. *Cell.* 77:627–638.

Sofroniew, M.V., C.L. Howe, and W.C. Mobley. 2001. Nerve growth factor signaling, neuroprotection, and neural repair. *Annu. Rev. Neurosci.* 24:1217–1281.

Sorkin, A., and M. Von Zastrow. 2002. Signal transduction and endocytosis: close encounters of many kinds. *Nat. Rev. Mol. Cell Biol.* 3:600–614.

Sweeney, S.T., and G.W. Davis. 2002. Unrestricted synaptic growth in spinster-a late endosomal protein implicated in TGF-β-mediated synaptic growth regulation. *Neuron.* 36:403–416.

Trajkovic, K., A.S. Dhaunchak, J.T. Goncalves, D. Wenzel, A. Schneider, G. Bunt, K.A. Nave, and M. Simons. 2006. Neuron to glia signalling triggers myelin membrane exocytosis from endosomal storage sites. *J. Cell Biol.* 172:937–948.

Umikawa, M., H. Obaishi, H. Nakanishi, K. Satoh-Horikawa, K. Takahashi, I. Hotta, Y. Matsuura, and Y. Takai. 1999. Association of frabin with the actin cytoskeleton is essential for microspike formation through activation of Cdc42 small G protein. *J. Biol. Chem.* 274:25197–25200.

van Niel, G., I. Porto-Carreiro, S. Simoes, and G. Raposo. 2006. Exosomes: a common pathway for a specialized function. *J. Biochem. (Tokyo).* 140:13–21.

Wu, C., C.F. Lai, and W.C. Mobley. 2001. Nerve growth factor activates persistent Rap1 signaling in endosomes. *J. Neurosci.* 21:5406–5416.

Wunderlich, W., I. Fialka, D. Teis, A. Alpi, A. Pfeifer, R.G. Parton, F. Lottspeich, and L.A. Huber. 2001. A novel 14-kilodalton protein interacts with the mitogen-activated protein kinase scaffold mp1 on a late endosomal/lysosomal compartment. *J. Cell Biol.* 152:765–776.

Yamada, T., T. Sakisaka, S. Hisata, T. Baba, and Y. Takai. 2005. RA-RhoGAP, Rap-activated Rho GTPase-activating protein implicated in neurite outgrowth through Rho. *J. Biol. Chem.* 280:33026–33034.

Yamamoto, T., K. Kaibuchi, T. Mizuno, M. Hiroyoshi, H. Shirataki, and Y. Takai. 1990. Purification and characterization from bovine brain cytosol of proteins that regulate the GDP/GTP exchange reaction of smg p21s, ras p21-like GTP-binding proteins. *J. Biol. Chem.* 265:16626–16634.

Yano, H., and M.W. Chao. 2005. Biochemical characterization of intracellular membranes bearing Trk neurotrophin receptors. *Neurochem. Res.* 30:767–777.

York, R.D., H. Yao, T. Dillon, C.L. Ellig, S.P. Eckert, E.W. McCleskey, and P.J. Stork. 1998. Rap1 mediates sustained MAP kinase activation induced by nerve growth factor. *Nature.* 392:622–626.

York, R.D., D.C. Molliver, S.S. Grewal, P.E. Stenberg, E.W. McCleskey, and P.J. Stork. 2000. Role of phosphoinositide 3-kinase and endocytosis in nerve growth factor-induced extracellular signal-regulated kinase activation via Ras and Rap1. *Mol. Cell. Biol.* 20:8069–8083.

Yoshimura, T., Y. Kawano, N. Arimura, S. Kawabata, A. Kikuchi, and K. Kaibuchi. 2005. GSK-3beta regulates phosphorylation of CRMP-2 and neuronal polarity. *Cell.* 120:137–149.

Zapf-Colby, A., and J.M. Olefsky. 1998. Nerve growth factor processing and trafficking events following TrkA-mediated endocytosis. *Endocrinology.* 139:3232–3240.

Zweifel, L.S., R. Kuruvilla, and D.D. Ginty. 2005. Functions and mechanisms of retrograde neurotrophin signalling. *Nat. Rev. Neurosci.* 6:615–625.